author comments on the manuscript "Monitoring CO emissions of the metropolis Mexico City using TROPOMI CO observations", reviewer 1

We would like to thank the reviewer for the constructive comments that aided us to improve our manuscript. In this document we provide our replies to the reviewer's comments. The original comments made by the reviewer are numbered and typeset in italic and bold face font. Following every comment, we give our reply. Here line numbers, page numbers and figure numbers refer to the original version of the manuscript, if not stated differently. Additionally, the revised version of the manuscript is added.

1 Major Comments

1. ***One of the main concerns is regarding the CO background concentration and chem- istry. Authors assume a time invariant CO background concentration, while I believe background processes in the region of interest and its surrounding are quite important. I highly suggest to describe in detail why a constant CO background has been used. Please explain in detail how the background CO flowing into the domain produced by all non-metropolis Mexico City (10 districts) sources, including, non-metropolis Mexico City fires, is treated. Considering the relatively long lifetime of CO transport is extremely important.***

   adjusted This is a misunderstanding, we are not assuming a time invariant CO background concentration in our study. Figure 2a shows for each TROPOMI overpass of Mexico City which background CO concentration was used. The time series clearly reflects elevated background CO concentrations during dry season (e.g. fire contribution) and low background CO during rainy season over Mexico City. Actually, we found, that the CO background concentration is a crucial component of our emission inversion scheme and therefore, decided to retrieve it together with the CO emission of the 10 city districts of Mexico (parameters $\alpha_{bg}, \alpha_{elev}$ in Equation 6). This ensures that the inversion scheme has the capability to decided itself which part of the TROPOMI measurement to interpreted as background and which as contribution from the city districts. Hence, all contribution from other sources excluding the 10 city districts will be represented by the fitted background parameters.
   To make this clearer, we changed the definition of the forward model in section 3.1. Now the background parameters are exclusively introduced as effective fit parameters in Eq. 5. Furthermore, we changed the paragraph p5, l27 from:
   " Finally, to improve the capability of the forward model to fit TROPOMI observations, we induce a linear altitude dependence of the simulated CO column $\mathbf{k}_{\mathrm{elv}} = z - z_{\mathrm{ref}}$. Here, z is the mean elevation in the TROPOMI CO ground pixels and $z_{\mathrm{ref}} = 2240$ m the reference altitude which is set to the elevation of Mexico City.

   $$\mathbf{F}_{\mathrm{sat}}(E_1, \cdots, E_{10}, \alpha_{\mathrm{bg}}) = \sum_{i=1}^{10} \mathcal{O}(\tilde{\mathbf{k}}_i)E_i + \mathbf{k}_{\mathrm{bg}}\alpha_{\mathrm{bg}} + \mathbf{k}_{\mathrm{elv}}\alpha_{\mathrm{elv}} \tag{5}$$

   With these additional degrees of freedom the forward model can mitigate shortcomings of the WRF simulations using a spatially constant CO background. "
   to
   " To improve the capability of our forward model to fit TROPOMI observations, we introduce a spatially constant CO background field $\mathbf{k}_{\mathrm{bg}}$ and an altitude dependence term $\mathbf{k}_{\mathrm{elv}} = z - z_{\mathrm{ref}}$ with corresponding scaling factors α_{bg} and α_{elv}. Here, z is the respective elevation of the TROPOMI CO ground pixels and $z_{\mathrm{ref}} = 2240$ m is an arbitrary reference altitude set to the elevation of Mexico City,

   $$\mathrm{F}_{\mathrm{sat}}(E_1, \cdots, E_{10}, \alpha_{\mathrm{bg}}, \alpha_{\mathrm{elv}}) = \sum_{i=1}^{10} \mathcal{O}(\tilde{\mathbf{k}}_i)E_i + \mathbf{k}_{\mathrm{bg}}\alpha_{\mathrm{bg}} + \mathbf{k}_{\mathrm{elv}}\alpha_{\mathrm{elv}}\ . \tag{5}$$

   "

2. ***Furthermore, biogenic non-methane VOCs emitted from vegetation might be important as a source for the chemical production of CO in the atmosphere. In the manuscript, I did not find information regarding these contribution, maybe it is too small for the metropolis?, what about the transport of the surroundings to the districts. It would be important to add a description on this.***

adjusted The WRF model in this study is run in transport only mode. Hence, the chemical production of CO is not accounted for. However, it should be small compared to the other sources. All type of contributions like this (biogenic) or from outside the domain such as fires, power plants, other cities as well as contribution from global CO is compensated by the fitted background parameters $\alpha_{bg}, \alpha_{elev}$. Hence, when the background CO field becomes too complex or inhomogeneous e.g. as discussed for the CO from wild fires in Fig. 3, our approach will fail to reproduce the TROPOMI measurements and these cases are rejected.
We changed the sentence p4,l14 from:
" Further, the forward model assumes linear dependence of CO background field $\mathbf{k}_{\mathrm{bg}}$ with scaling parameter α_{bg} . . . "
to
" These two effective model components account for CO contribution over the Mexico City area originating from outside the model domain such as fires, power plants, biogenic production, other cities as well as the long-range transport (Borsdorff et al., 2019) and an altitude dependent linear vertical gradient of the CO columns. Both do not interfere with any localized emission sources. They mitigate shortcomings of the WRF-chem simulations ignoring CO boundary conditions at the model domain. "

3. ***Lastly, according to the authors the configuration of the model does not account for atmospheric chemistry, does that mean that Gas-phase Chemistry is not included?. Similarly, please include a description of why this configuration was chosen.***

   adjusted

   We changed the sentence p3,l29 from:
   " . . . and does not account for atmospheric chemistry (Dekker et al., 2017)."
   to
   " We ignore photo-chemical oxidation and secondary production of CO in the atmosphere (chem_opt option 106 (RADM2-KPP), as a tracer with gaschem off), which is justified by the long lifetime of CO compared with the size of the model domain as discussed by Dekker et al. (2017). Especially, for the region of Mexico City the contribution of atmospheric chemistry to the total CO concentration is less than 3% as presented by Mejia (2020). Hence, WRF-chem simulates the transport of CO surface emission as traces as done by e.g. Borsdorff et al. (2019), Dekker et al. (2017, 2018). "

2 Specific Comments

1. ***Authors recognize the possible error sources, and if I understand correctly authors estimate uncertainties in the inversion, I highly suggest to include the uncertainties of emissions in the abstract.***

   adjusted

   We changed the sentence p1,l8 from:
   " . . . 0.10 Tg/yr and 0.08 Tg/yr CO"
   to
   " 0.10 ± 0.004 Tg/yr and 0.09 ± 0.005 Tg/yr CO "

   We changed the sentence p1,l10 from:
   " For CDMX, TROPOMI estimates emissions of 0.14 Tg/yr . . . "
   to
   " On the other hand for Ciudad de Mexico, TROPOMI estimates emissions of 0.14 ± 0.006 Tg/yr CO, . . . "

   We changed the sentence p1,l11 from:
   " ACDMX area, however, has a higher emissions with 0.29 Tg/yr according to TROPOMI observations . . . "
   to
   " . . . Arena Ciudad de Mexico the emission is 0.28 ± 0.01 Tg/yr according to TROPOMI observations . . . "

   We changed the sentence p1,l10 from:
   " . . . (0.43 Tg/yr TROPOMI versus 0.39 Tg/yr adapted INEM emissions). "
   to
   " . . . (0.42 ± 0.016 Tg/yr TROPOMI versus 0.39 Tg/yr adapted INEM emissions)."

In addition we changed the same statements in the results and conclusion section p8,l30-43.

2. ***P1, L2. It is mentioned that 551 overpasses are analyzed, please specify the exact time period. The season(s) might be relevant.***

   adjusted

   We changed the sentence p1,l2 from:
   " . . . (more than 2 years of measurements) using . . . "
   to
   ". . . we analyze TROPOMI observations over Mexico City in the period 14 November 2017 to 25 August 2019 by . . . "

3. ***P1, L4. It is not clear to me if you use WRF coupled with Chemistry (WRF-Chem)?***

   adjusted

   We changed the sentence p1,l4 from:
   " . . . regional Weather Research and Forecasting (WRF) model to conclude . . . "
   to
   " . . . regional Weather Research and Forecasting (WRF-chem) model to conclude . . . "

   Accordingly, we changed the Acronym in the whole document

4. ***P1, L8. Do you identify the sources missing in the INEM in Tula and Pachuca?***

   adjusted

   We added the following sentence p8,l30:
   " It is not yet clear what sources are missing in the inventory, this needs to be addressed in future studies. However, we identified an oil refinery and a power plant near to Tula and cement and lime kilns near to Pachuca that could contribute to the CO emissions. "

5. ***P1, 14. It is mentioned: "CDMX and ACDMX follow a clear weakly cycle with a minimum during the weekend" does this mean that the weekend effect is not found in the other regions?***

   not adjusted

   No, but we cannot not conclude on it yet. We need to wait for more TROPOMI data to analyze the remaining districts.

6. ***Section2, TROPOMI CO data set: In the current manuscript, I do not find a real value of including the FTIR observations, however it might be good to include it in this section. I suggest to include comparisons between TROPOMI and FTIR for coincident dates, do they compare ok?***

   not adjusted The agreement between TROPOMI and the FTIR measurements is already analyzed in Borsdorff et al. (2018). We found in general a good agreement with a low bias. The FTIR measurements show that the weekly cycle in CO can be detected in the total column concentration and by that adds extra information to weekly cycle that is detected by in-situ measurements at the surface. Hence, we would like to keep the FTIR measurements here.

7. ***Section 3.1, The WRF model. Important chemical parameterizations in the model are missing, e.g., what biogenic and biomass burning emissions are used?. What kind of boundary conditions?. Is the inflow of CO emitted by fires outside the region of interest included?. What time step is used?***

   adjusted

   We added the following sentence p3,l29:
   ". . . (chem_opt option 106 (RADM2-KPP), as a tracer with gaschem off) . . . "

   Please also see major comment 3 of referee 1.

8. ***P4, L17. Do you mean equation 1?***

   corrected

9. ***P5, L3-7. As in my major comment, it is a big assumption that local enhancements of CO are due to emissions of the city districts of the same day with a constant CO background?. It is well known that biomass/fire emissions can contribute significantly to the CO in the region. I wonder why an inflow of background CO is not taken into account, my understanding is that WRF-Chem can handle this.***

   adjusted

   Please also see our answer to the major comment of the referee. We changed the paragraph p5,l3-7 from:
   " In our simulation of TROPOMI CO observations, we assume that the local enhancements of CO are due to emissions of the city districts of the same day, whereas emissions from outside the domain as well as the temporal accumulation of CO emission of the domain is described by the background CO field. Therefore, it means that the inferred emissions E_i represents an emission estimate of the urban district for the particular observation day. Moreover, the effective model parameter α_{bg} and α_{elv} may vary between different TROPOMI overpasses.
   to
   " Finally, for the interpretation of our CO forward simulations, we make an important assumption. Although the WRF simulations account for the temporal accumulation of the localized CO emission over days and weeks, we allocate an emission estimate of the corresponding overpass time to each TROPOMI overpass. Here, we assume that a TROPOMI CO image is dominated by the emissions of the urban districts for the particular observation day, where the temporal accumulation of CO from previous days is partly described by the WRF simulation due to the corresponding scaling of the inventory and partly mitigated by fitting the nuisance parameter α_{bg} and α_{elv}. "

10. ***In order to have a sense of the spatial distribution of CO, I highly suggest to include the urban districts in Fig. 3.***

    adjusted The figure is updated as suggested.

11. ***P8, L2-9. It is not clear how the background concentration was estimated.***

    adjusted

    We changed the sentence p8,l1 from:
    " Fig. 2 shows the fitted CO background concentration and its annual cycle."
    to
    " Fig. 2 shows the CO background that was fitted as an auxiliary parameter during the inversion described in Sec. 3.2. The concentration and its annual cycle is shown. "

12. ***P8, L9. It is mentioned that the fire season many data cannot be considered, how many days (or percent) are excluded based on this?***

    adjusted

    We changed the sentence p8,l9 from:
    " Only fitting a scaling to a constant background field is not sufficient in this extreme cases and so during the fire season many data cannot be considered. . . . "
    to
    " Only fitting a scaling to a constant background field is not sufficient in these extreme cases and so during the fire season many data cannot be considered (we excluded the month May and June 2019). "

13. ***Figure 4, It is hard to identify the districts on this figure, maybe you could include the contour/shapes of the districts.***

    adjusted

    The figure is updated as suggested.

14. ***Figure 5. I recommend to follow the names of the districts as in Figure 1. Especially for Ciudad de Mexico and CDMX.***

    adjusted

    We updated Fig. 5,6,7, and 8 as well as the whole text of the Manuscript. The term "Ciudad de Mexico" is replaced by ACdMx and "CDMX" by "CdMx". Hence, we are now following the nomenclature shown in Figure 1.

15. ***Figure 5. why does Tulancingo have a zero emission?***

    adjusted

    We changed the sentence p9,l11- from:
    " Moreover, the averaging kernel shows that the Final-fit inversion is insensitive to deviations of the Tulancingo emission from the prior estimate. Whereas the Pre-fit inversion estimates very small emissions for this district, the subsequent regularization changes the emission only marginally. "
    to
    " The figure shows that generally the averaging kernels have high values on the diagonal indicating high sensitivity to the quantity to be retrieved. It indicates that TROPOMI measurements can be used to distinguish emissions of the different urban districts of Mexico, with the exception of the emissions of district Tulancingo. Due to the small mean emission, the averaging kernel indicates a low sensitive of the data product. "

16. ***Figure 5. Is the number of collocations the same as the number of days?***

    adjusted

    We added the following sentence to Figure 5:
    " Here, a collocation corresponds to a specific day because TROPOMI overpasses the region only once. "

17. ***Figure 7. what does negative CO emission mean?***

    adjusted

    We added the following sentence p9,l25:
    " The scatter of the data is still high and even includes negative values. Even though negative emissions are not physical we need to keep them in our analyzes because filtering negative noise can induce a positive bias in the mean. "

18. ***Figure 7. It is hard to believe that emissions on Sat and Sunday are very similar, what time does it represent the emissions?***

    adjusted

    We added the following sentence p9,l29:
    " We found that the CO values on Saturday and Sunday are equally low. An explanation for this could be that the main source of CO in Mexico City during the week is traffic which is responsible for the weekly cycle and the remaining sources like cooking, water heating, etc. should not change much during the weekend. "

19. ***Figure 8. The weekly cycle of CO is considerably different than the weekly cycle of the emissions from Fig 7 (c), maybe I miss it but do you explain why?. Also, error bars from FTIR are extremely low, I do not think a standard deviation from the mean is the best way to characterize variability.***

    not adjusted

    We discussed this point on p9, l34. The variability of the weekly cycle is to high to conclude on its form yet. This will be revisited when we have more TROPOMI CO data available.

References

Borsdorff, T., aan de Brugh, J., Hu, H., Hasekamp, O., Sussmann, R., Rettinger, M., Hase, F., Gross, J., Schneider, M., Garcia, O., Stremme, W., Grutter, M., Feist, D. G., Arnold, S. G., De Mazière, M., Kumar Sha, M., Pollard, D. F., Kiel, M., Roehl, C., Wennberg, P. O., Toon, G. C., and Landgraf, J.: Mapping carbon monoxide pollution from space down to city scales with daily global coverage, Atmospheric Measurement Techniques Discussions, 2018, 1–19, https://doi.org/10.5194/amt-2018-132, URL `https://www.atmos-meas-tech-discuss.net/amt-2018-132/`, 2018.

Borsdorff, T., aan de Brugh, J., Pandey, S., Hasekamp, O., Aben, I., Houweling, S., and Landgraf, J.: Carbon monoxide air pollution on sub-city scales and along arterial roads detected by the Tropospheric Monitoring Instrument, Atmospheric Chemistry and Physics, 19, 3579–3588, https://doi.org/10.5194/acp-19-3579-2019, URL `https://www.atmos-chem-phys.net/19/3579/2019/`, 2019.

Dekker, I. N., Houweling, S., Aben, I., Röckmann, T., Krol, M., Martínez-Alonso, S., Deeter, M. N., and Worden, H. M.: Quantification of CO emissions from the city of Madrid using MOPITT satellite retrievals and WRF simulations, Atmospheric Chemistry and Physics, 17, 14 675–14 694, https://doi.org/10.5194/acp-17-14675-2017, URL `http://dx.doi.org/10.5194/acp-17-14675-2017`, 2017.

Dekker, I. N., Houweling, S., Pandey, S., Krol, M., Röckmann, T., Borsdorff, T., Landgraf, J., and Aben, I.: The origin of CO sources during the 2017 high pollution episode in India determined with TROPOMI and WRF data, manuscript in prep., 2018.

Mejia, J. F.: Running WRF in an Atmospheric Modeling Class: challenges and learning experiences, Atmosfera, 2020.

author comments on the manuscript "Monitoring CO emissions of the metropolis Mexico City using TROPOMI CO observations", reviewer 2

We would like to thank the reviewer for the constructive comments that aided us to improve our manuscript. In this document we provide our replies to the reviewer's comments. The original comments made by the reviewer are numbered and typeset in italic and bold face font. Following every comment we give our reply. Here line numbers, page numbers and figure numbers refer to the original version of the manuscript, if not stated differently. Additionally, the revised version of the manuscript is added.

1 General Comments

1. ***two-step minimization: The optimization of the emissions requires two steps. The first step (pre-fit) filters out a significant fraction of the TROPOMI data based on several criteria, while the second step (final fit) includes the entire data set. Some of these criteria require more justification, especially when threshold values are bieng used without any justification.***

   adjusted

   We relaxed the filter criteria for the Pre-fit retrieval and by that were removing the criteria criticized by the referee. The changes in our results are insignificant (please see the attached Fig.1 for a comparison). Accordingly, we recalculated everything and changed all the resulting numbers in the manuscript. The description of the filter criteria (p6,l23- p7l5) is changed from:
   " (3) The quality of the forward model depends on the meteorological situation, where we consider model simulations for low wind speeds more reliable. This considerations led to the criteria of the data filtering for the pre-fit. Thus, we only select overpasses which meet all of following filter criteria:

   - 70 % of the data domain is covered by TROPOMI observations
   - for all observations the across track pixel size is < 15 km.
   - the average wind speed of the scene is < 4 m/s.
   - The fit residuum $\langle\delta\rangle < 8$ppb, and the standard deviation $\sigma(\delta) < 8$ppb to limit the effect of too large forward model errors.
   - $\sigma(\delta)/\delta(\mathbf{y}_{\mathrm{meas}}) < 0.65$ to ensure that the forward model can explain the variability of the measured CO field.
   - $\sigma(\mathbf{F}(\mathbf{x})) > 4$ ppb to ensure that the model data contain a clear pollution signatures.
   - the Pearson correlation coefficient $r > 0.3$ between $CO_{TROPOMI}$ and CO_{WRF}.

   The filter criteria reduce the original set of 551 overpasses to 148, which we consider to be sufficient to estimate the overall average emission rate per district, yielding the prior state vector $\mathbf{x}_a$. "
   to
   " These considerations led to the criteria of the data filtering to determine the mean emission for each district. We only select overpasses which meet both filter criteria:

   - 70 % of the data domain is covered by TROPOMI observations
   - for all observations the across track pixel size is < 15 km.

   The filter criteria reduce the original set of 551 overpasses to 199, which we consider to be sufficient to estimate the overall average emission rate per district, yielding $\bar{x}$. "

   The statement of the referee about the optimization is addressed in the following comment.

2. ***But more importantly, this two-step process implies that the same measurements have been used twice. This approach seems to be a solution to the noise affecting the model-data residuals, hence limiting the convergence of the optimization system. In figure 5, there is almost no difference between the pre-fit and the final fit. The results are already constrained after the pre-fit step, except that the error bars further decrease, which seems artificial without assimilating additional measurements. To be clear, data should never be used twice in the optimization as it artificially in- creases the information content from the data set. Instead, the emissions should be produced by a single optimization procedure, iterative or at once, but extracting infor- mation only one time. If the noise is the inherent problem here, it***

should be treated by filtering out the noise in the data or in the model. Smoothing data signals, decom- posing the signals into frequencies, or averaging over time (both model and data) will help extract the information from noisy model-data residuals. Other approaches like Wasserstein distance or other machine learning techniques will help remove the noise. The optimization procedure needs to be revised to produce robust emissions and un- certainties. As it stands, the selection of data is arbitrary and the optimization uses the sae data multiple times.

adjusted

We completely rewrote section 3.2 about the inversion methodology (please see the new version of the manuscript). Our aim is to show that our two-step inversion scheme is extracting orthogonal information from the measurements and by that not the same information is extracted twice. "

3. ***Background determination: The determination of the background CO values is never explained in details. The first paragraph of Section 4 describes very briefly that CO background has been fitted. Which domain has been used? The entire State of Mex- ico? Considering the topography, the gradients over the domain, and the potential contamination by other sources (such as fires, but also cities, industries, shipping, . . .), the uncertainty associated with the background determination needs to be quanti- fied and included in the optimization. The uncertainty associated with the background seems to be equal to zero in the final fit (section 3.4). How is the uncertainty defined in the optimization? Zero values appear in the prior error covariance matrix (P7-L14). It suggests that the background is pre-defined (before the final optimization). A section should describe precisely how the background values are determined in (or before) the optimization. Assuming you provide a coherent one-step minimization procedure, and a robust de- termination of th background values for each day, I recommend that you include some pseudo-data experiments to evaluate the potential of your optimization to constrain the city emissions. Simple perturbations should be added to urban districts to determine the actual constraint from TROPOMI data.***

   adjusted

   In our approach we chose to infer information about the background CO directly from the TROPOMI CO measurements by simultaneously fitting the parameters ($\alpha_{\mathrm{bg}}, \alpha_{\mathrm{bg}}$) of Eq. 5) together with the emission estimates of the different city districts in the same domain. This is advantageous because the inversion can decide itself which part of the measured signal is classified as background and which as pollution from the city districts which minimized the change to introduces biases in the emission estimates. For the same reason we are fitting the background parameters always without imposing a regularization for each TROPOMI orbit. Here, the parameter α_{bg} models a background CO concentration and α_{bg} a gradient of the vertical CO concentration dependent on the orography of the region.
   Please see our answer to the third major comment of referee 1 and the corresponding changes to the manuscript.
   The zeros in the regularization matrix ensure that the background parameters are not regularized. To make this more clear We change the sentence p7,l14:
   from
   " such that the elements of the state vector $\alpha_{\mathrm{b}g}$ and α_{elv} are not regularized. "
   to
   " . . . where the zeros ensure that the elements of the state vector α_{bg} and α_{elv} are not regularized. Obviously, the . . . "
   Furthermore, the errors of the background are shown in Fig.2 for each point. They are small because we have a strong signal about the background in the TROPOMI data.

4. ***As a last comment, the selection of data with low wind speed conditions will increase the model errors. If the aboslute wind speed is 2 m/s, an error of 2 m/s in wind speed corresponds to an error of 100% on the emissions. It maximizes the local enhance- ments which helps with the large noise, but this filter is typically the opposite in most studies using satellite data (minimum wind speed). Removing noise will help removing that threshold which seems to be a simple but risky solution to reducing the noise in model-data residuals.***

   adjusted

   Please see our answer to the first mayor comment of the referee. In the new version of the manuscript we will not filter on the wind speed anymore. We found removing these filter criteria have no significant effect on our results (see the attached Fig. 1).

2 Technical Comments

1. ***P2 L1: and its transport in the atmosphere : Unclear.***

   adjusted

   We changed the sentence p2,l1 from:
   " These characteristics established CO as a tracer for air pollution and its transport in the atmosphere . . . "
   to
   " These characteristics established CO as a tracer for air pollution and transport processes in the atmosphere "

2. ***P2 L20: Add references for the error sources***

   adjusted We added a reference to (Borsdorff et al., 2019) where we discussed the errors on the example of pollution transport from Tehran.

3. ***P2 L30: Here the emission estimation changed by 0.42 Tg/yr 30 in only 2 years from 2014 to 2016, due to a change in the mobile emission model from mobile to moves. This means that the emission model changed and not the emissions. Has this change been confirmed or validated by other data?***

   adjusted

   We haven't found a validation or confirmation of this. However, it shows that the error bars on the emissions of the INEM inventory are big. To prevent confusions, we removed the sentence.

4. ***P4 L5: The inventory is time dependent and accounts for the diurnal, week-to-week and monthly variations of the emissions How accurate are these cycles? Considering the overpass time is fixed, the mismatch can be explained by a difference in diurnal cycles in and out of the city. How was the inventory constructed? Does it include traffic counts? Are the other sectors using temperature-dependent relationship?***

   adjusted

   There are no sectors using temperature-dependent relationships in the inventory. We are adding the following sentence at p4, l5:
   " The weekly and daily mobile temporal profiles are derived from traffic counts in Mexico. The emissions inventory is described in Garcia et al. (2018). "
   We added the following sentence at p11,l10:
   " Another potential error source of our method are the accuracy of the week-to-week and monthly variations of the emissions in the INEM inventory considering the fixed overpass time of TROPOMI."

5. ***P4 L29: Here, z is the mean elevation in the TROPOMI CO ground pixels and zref = 2240 m the reference altitude which is set to the elevation of Mexico City. This correction is unclear. The altitude used by TROPOMI is defined as a surface pressure. The altitude error depends on the difference between the WRF surface pressure and the TROPOMI surface pressure. Why using an average altitude of Mexico City as a reference?***

   adjusted

   Actually, the reference altitude can be arbitrary chosen. However, we selected a altitude that is in the range of our region of interest. We change the sentence at p4, l29 from:
   " Here, z is the mean elevation in the TROPOMI CO ground pixels and $z_{\mathrm{ref}} = 2240$ m the reference altitude which is set to the elevation of Mexico City. "
   to
   " Here, z is the respective elevation of the TROPOMI CO ground pixels and $z_{\mathrm{ref}} = 2240$ m is an arbitrary reference altitude set to the elevation of Mexico City, . . . "

6. ***P5 - L4: local enhancements of CO are due to emissions of the city districts of the same day Have you tested that assumption? Basin cities are often problematic with low wind speed for days, which can accumulate signals from more than one day in the basins (example: Los Angeles during Winter). An averaged wind speed or residence time of tracers would help justify this assumption.***

   adjusted

   We added the following sentence at p11,l10: " Furthermore, basin cities can be problematic with low wind speed for days, which could lead to accumulate signals from more than one day in the basins which is not yet covered by our approach. To account for this effect in our inversion needs major adjustments, which will be investigated in follow up studies. "

7. ***P5: Use the current notation for multivariate regression used in most publications (observation operator H, state vector x, prior error cov B, Obs error cov R, observations y, Kalman gain K).***

   not adjusted

   We are using the notation of Rodgers (2000) that is commonly used in our field.

8. ***P6 - L17: with little forward model errors. Unclear. Re-phrase.***

   adjusted

   We changed the sentence p6,l17 from:
   " On one hand, it should be large enough to estimate mean emissions for the period of TROPOMI observations, and the other hand strict data filtering is required to get a stable inversion with little forward model errors"
   to
   " On the one hand, the ensemble should be large enough to estimate mean emissions for the considered time period, but on the other hand it should be strictly filtered for cases where the forward model is in good agreement with the measurement such that a stable inversion of the all emissions is possible. "

9. ***P6 L24: for low wind speeds more reliable. The model errors are critical during low wind speed conditions when a slight change in wind speed can affect the magnitude of the observed enhancements. Typically, high wind speeds should be avoided because local enhancements are weak while low wind speeds should also be avoided when a small change in the wind speed can significantly change the local enhancements.***

   adjusted

   Please see our answer to the first mayor comment of the referee. In the new version of the manuscript we will not filter on the wind speed anymore. We found removing this filter criteria has no significant effect on our results (see the attached Fig. 1).

10. ***P6 L30: fit residuum ¡ 8ppb, and the standard deviation ¡ 8ppb to limit the effect of too large forward model errors. TROPOMI is an averaged enhancement over a grid cell. Point sources will be under-estimated in the data as the plume will not be mixed over the entire grid cell. This bias has been presented by the TROPOMI team. Can you conform the relationship between point sources over the domain and the location of these high model-data differences?***
    In addition, removing noisy pixels will artificially decrease the uncertainty by removing undesirable pixels. Some of these large model-data differences might be real transport errors or observation noise.

    adjusted

    The under-estimation reported by the TROPOMI was analyzed for point-sources smaller than a TROPOMI pixel deploying the mass balance method. This does not hold here, we are looking at city districts that in general extend over multiple TROPOMI ground pixel (see Fig. 4 of the old manuscript).
    The filter criteria criticised by the referee is not applied anymore in the new version of the manuscript. Please have a look at our answer to the first major comment of the reviewer. Removing this criteria was not changing our results significantly (see the attached Fig. 1).

11. ***P7 L1: . . . (ymeas) ¡ 0.65 to ensure that the forward model can explain the vari- ability of the measured CO field. This value seems arbitrary. How did you define it?***

adjusted

Please see our answer to the first mayor comment of the referee. In the new version of the manuscript we will not apply this filter anymore. We found removing this filter criteria has no significant effect on our results (see the attached Fig. 1).

12. ***P7 L4: What I the impact on the seasonal distribution? Does it remove data evenly over the year? This filters are likely to bias your results over specific season. A figure showing the time depencen of the filtered data is needed (or statistics)***

adjusted

Please see the major comment one of this referee. We removed many of this filters and our results are still stable. However, an even sampling over all seasons is not use full here. We described in p8l1-9 that in particular measurements during the biomass burning season are too difficult to interpret with our method and should be rejected to ensure data quality.

13. ***P7 L15: Kbg and Kelv are not regularized How can you optimize the emissions without regularizing the background values? Are they pre-determined? How were they defined?***

adjusted

The signal about the background parameters is very strong. The parameters are fitted without regularization for each overpass of TROPOMI. Please see the major comment of referee 1.

14. ***P7 15-20: The balance between prior information and data constraint is usually computed with the Chi2 normalized distance. A value near one will define the optimal balance between the two. Michalak, A., Hirsch, A., Bruhwiler, L., Gurney, K., Pe- ters, W., and Tans, P.: Maximum likelihood estimation of co- variance parameters for Bayesian atmospheric trace gas sur- face flux inversions, J. Geophys. Res.-Atmos., 110, D24107, https://doi.org/10.1029/2005JD005970, 2005.***

not adjusted

A major problem we are facing in this study is that the priori information from the INEM inventory seems to be biased. Hence, we don't want to constrain our inversion to much by it.

15. ***P7 L21-24: This approach weighs toward pixels that are co-located with the sources. In other words, it selects preferentially the pixels above the city. In general, it should work but an evaluation perido would be helpful (with and without the filter) to measure the impact of the selection. This approach might bias the results if the model under- /over-estimate urban pixels.***

not adjusted

When we don't apply the regularisation the inversion depends on forward model errors what we showed in this study.

16. ***P7 L23: temporal variation of the INEM emissions to be about 40%***

. . .

vary with 60% around their average How do you define the 60%? The link between 4060% is not explained. In addition, temporal variations and mean emission errors are not supposed to scale together. This part needs to be described more carefully. The emission errors should depend on the emissions alone instead of their temporal vari- ability.

adjusted

The value 60% was chosen to not over regularize the inversion. Hence, we could of course enforce 40% here but this choice is a balance between propagation of errors and extraction of information content from the measurement. To make this more clear, we change the paragraph at p7,l22 from:

" Considering the temporal variation of the INEM emissions to be about 40%, we adjusted the regularization parameter $\gamma_1, \cdots, \gamma_{10}$ such that the retrieved emissions vary with 60% around their average. Hence, our regularization is not enforcing that the retrievals show the same variability as the emissions of the inventory. The value 60% is an empirical parameter which the retrieval more freedom to balance information content and noise propagation. This puts a moderate constraints on the inversion ensuring on one hand a stable inversion and on the other hand a realistic variation of the retrieved emissions around the priori. "
to

" Considering the temporal variation of the INEM emissions to be about 40%, we adjusted the regularization parameter $\gamma_1, \cdots, \gamma_{10}$ such that the retrieved emissions vary within 60% around their average. The value 60% is empirical chosen to balance information content against noise propagation. It puts a moderate constraints on the inversion ensuring on the one hand a stable inversion and on the other hand a realistic variation of the retrieved emissions around the priori. "

17. ***Figure 4: This figure provides illustrations but is not very helpful to prove that the WRF model is reliable or good enough. Instead, model-data mismatches should be pre- sented in a synthetic figure, for different times of year, using whisker boxes. Snapshots for four days out of 160 is too few to convince the readers. This figure should be replaced.***

    adjusted

    We disagree. We think that this examples clearly show the advantages and limitations of our our approach as we also discuss it in the manuscript.

18. ***P8 L18: This clearly shows that regional models like WRF have a great potential for the interpretation and analysis of TROPOMI data. No, this does not demonstrate the model capabilities nor the ability fo the model to extract emissions. Re-phrase.***

    adjusted

    We changed the sentence p8,l18 from:
    "This clearly shows that regional models like WRF-chem have a great potential for the interpretation and analysis of TROPOMI data. "
    to
    " This clearly shows that regional models like WRF-chem have a great potential to reproduce the large-scale patterns seen by the TROPOMI instrument. "

19. ***P8 L21: For atmospheric conditions under high wind speeds the WRF simulations can deviate more from the TROPOMI measurements as shown in Fig. 4 (c). This single day is too limited to conclude anything. More statistics on windy days are needed to prove your point is valid here.***

    adjusted

    The aim of the study is not to analyze model error under high wind speeds. Please have a look at our answer of the major comment of referee 1. We removed the filtering on wind speed and our results were not changing significantly (see the attached Fig.1)

20. ***Figure 5: The modeled and observed XCO should be presented first, summarized for the days available before and after filtering. Do the residuals show a seasonality? The results of the optimization are difficult to interpret without the evaluation of the initial model results.***

    not adjusted

    The comment is not well formulated and we don't understand it.

21. ***P9 L1-6: Large model-data mismatches are expected from observations, model er- rors, and prior errors. If observations are being used twice (if I understood correctly), mismatches will decrease automatically. Optimization should never be performed a second time with the same data. Unless I misunderstood the approach (different data are being used between these two steps), only one step should be performed. Other- wise the constraint from the data is over-estimated.***

adjusted

Please see our answer to the major comment two of the referee.

22. ***P9 L7: Furthermore, non-uniform variation of the background CO concentration can be a additional reason for this scatter (as shown in Fig. 3). How did you determine the background? How do you separate the contribution from the city emissions? Is it all performed within the inversion? If so, how do you define background uncertainties? Some additional tests should be performed. If you introduce a background in the bias, is your optimization system able to recover that bias? Figure 6: statistics should be presented for the entire data set and not only for four days.***

adjusted

The background parameters are retrieved together with the emission estimates from the measurements of each TROPOMI overpass. Please have a look at the major comment of referee 1 were we adapted the manuscript accordingly. Fig. 2 of the old manuscript shows for each TROPOMI measurement the inverted background values together with the retrieval errors represented as error bars. However, it is for sure also important to analyze individual cases like shown in Fig.5 because not every issue becomes visible when looking at statistics. We tested our inversion routines and they are working. Hence, introducing and retrieving an artificial background is not helping further here.

We added a sub-figure in Fig.6 showing the goodness of the fit between TROPOMI and WRF for the priori emissions, the ones of the Pre-fit and Final. We changed the paragraph p6, l3-8 from:

“ This yields the mean

$$\langle\delta\rangle = \frac{1}{J}\sum_{j=1}^{J}\delta_j \tag{13}$$

and the standard deviations of the residuals

$$\sigma(\delta) = \frac{1}{J-1}\sum_{j=1}^{J}(\delta_i - \langle\delta\rangle)^2 \tag{14}$$

The standard deviation $\sigma(\mathbf{y}_{\mathrm{meas}})$ and $\sigma(\mathbf{F}(\mathbf{x}))$ of the TROPOMI CO field and the corresponding WRF-chem forward simulation completes our set of diagnostics.

”

to

“ To evaluate the fit quality for each overpass, we consider the fit residuals $\delta_i = y_i - \mathbf{K}_i x_{\mathrm{est},i}$. Additionally, we evaluate the goodness of the fit described by the reduced chi squared value,

$$\chi_i^2 = \frac{1}{\nu_i}\sum_{l=1}^{L}(\delta_i, l/y_{\mathrm{err},ik})^2 \,. \tag{22}$$

Here L is the number of observation of a single overpass, $y_{\mathrm{err},i}$ the retrieval error, and $\nu_i = L - \mathrm{DFS}_i$. ”
We changed the caption of Fig.6 from:
“ . . . as a robust estimation of the standard deviation and the number of collocations (c). The number of collocation of the Pre-fit is the same for all tracer domains (blue line) but in the Final-fit it is changing due to the information content filtering. Here, a collocation corresponds to a specific day because TROPOMI overpasses the region only once.
”
to
“ . . . as a robust estimation of the standard deviation, (c) the median of the goodness of the fit (χ^2), and the number of collocations (d). The number of collocations and the χ^2 values of the apriori simulation and Pre-fit are the same for all tracer domains (blue and grey line) but in the Final-fit it is changing due to the information content filtering. Here, a collocation corresponds to a specific day because TROPOMI overpasses the region only once. ”
We added the discussion at p9,l9:
“ The χ^2 values in Fig. 6 clearly show that the agreement between TROPOMI and WRF can be improved by fitting the emissions of the different city districts (blue line) instead of using the INEM inventory (grey

line). The regularization approach increases the χ^2 values (green bars) because the inversion can less compensate differences between TROPOMI and WRF by choosing unrealistic emissions. However, the χ^2 values of the Final-Fit are still lower than the ones for the prior INEM emissions (grey line). Overall, the χ^2 values exceeds 1 which indicates that the difference between TROPOMI and WRF is dominated by systematic errors in the WRF simulation. "

23. ***P9 L13-14: the averaging kernel shows that the Final-fit inversion is insensitive to deviations of the Tulancingo emission from the prior estimate. Whereas the Pre-fit inversion estimates very small emissions for this district, the subsequent regularization changes the emission only marginally. This is the direct consequence of performing an optimization with the same data twice. Some of the constraint has already been introduced in the emissions.***

    adjusted

    Please also see our answer to the major comments of the referee. The idea of the Pre-fit is to estimate mean emissions for all regions to prevent biases due to imposing a regularization. Hence, we want that the emissions of the Pre-fit and Final are the same.

    We change the sentence at p9, l14 from:
    " Moreover, the averaging kernel shows that the Final-fit inversion is insensitive to deviations of the Tulancingo emission from the prior estimate. The reason for this is that the Pre-fit inversion was only estimating very small emissions for this district and the regularization of the Final-fit is changing this only marginally. "
    to
    " It indicates that TROPOMI measurements can be used to distinguish emissions of the different urban districts of Mexico, with the exception of the emissions of district Tulancingo. Due to the small mean emission, the averaging kernel indicates a low sensitive of the data product. "

3 Special Comments

1. ***Specific comments: P6 L15: depends crucially = highly depends on***

    corrected

References

Borsdorff, T., aan de Brugh, J., Pandey, S., Hasekamp, O., Aben, I., Houweling, S., and Landgraf, J.: Carbon monoxide air pollution on sub-city scales and along arterial roads detected by the Tropospheric Monitoring Instrument, Atmospheric Chemistry and Physics, 19, 3579–3588, https://doi.org/10.5194/acp-19-3579-2019, URL `https://www.atmos-chem-phys.net/19/3579/2019/`, 2019.

Rodgers, C. D.: Inverse methods for atmospheric sounding: theory and practice, vol. 2 of *Series on atmospheric, oceanic and planetary physics*, World Scientific, Singapore, River Edge, N.J., reprinted : 2004, 2008, 2000.

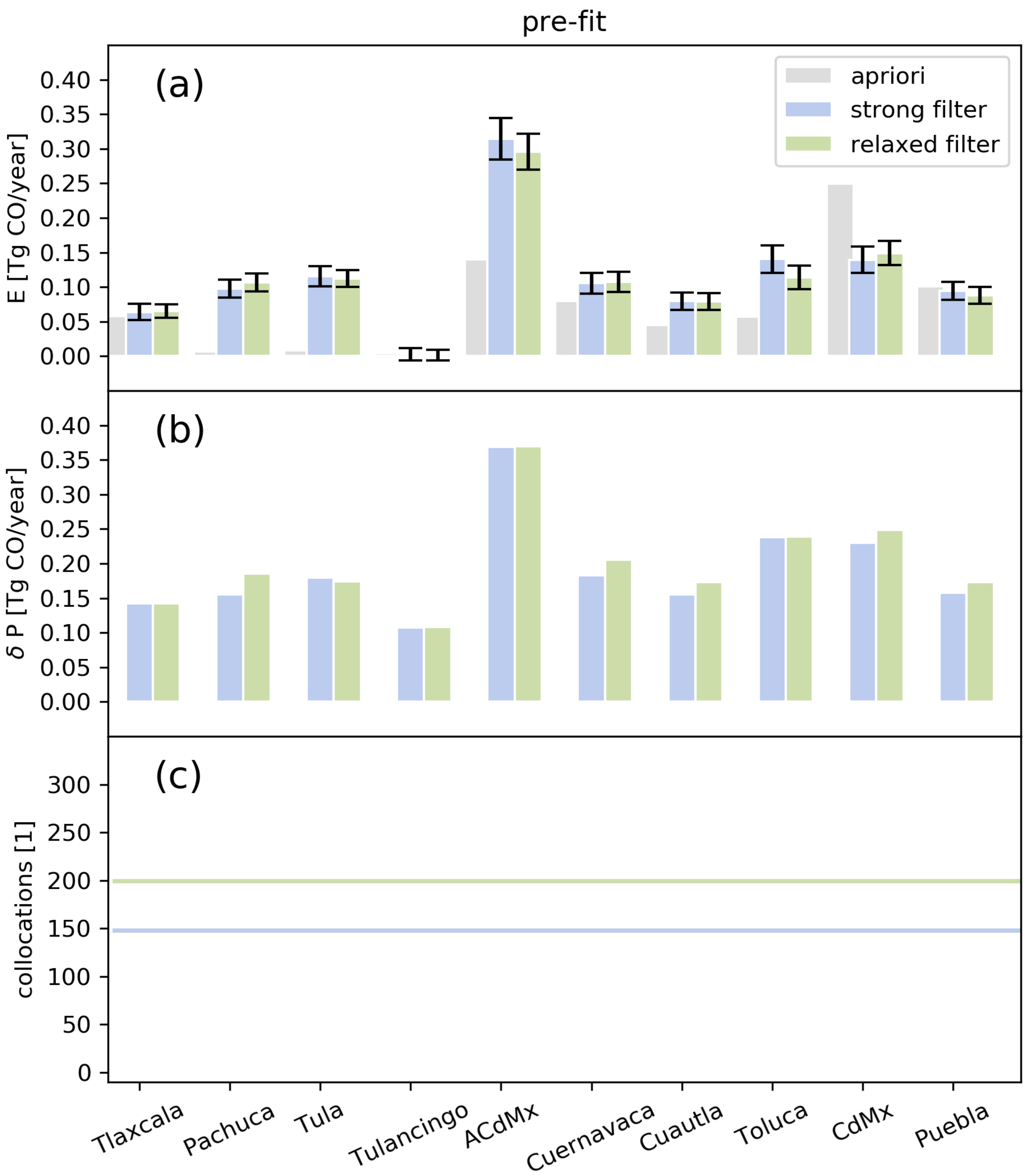

Figure 1: Statistics of CO emissions averaged from the 9th of November 2017 to the 25th of August 2019 for the tracer domains shown in Fig.1. (a) Median of the priori emissions (adapted INEM inventory) used for the WRF-chem simulation (grey) and retrieved from the TROPOMI data (Pre-fit in blue, Prefit-fit with relaxed filtering in green). The error bars indicate the standard error of the mean calculated from the delta percentiles (b) used as a robust estimation of the standard deviation and the number of collocations (c). The number of collocation of the Pre-fit is the same for all tracer domains (blue and green line). Here, a collocation corresponds to a specific day because TROPOMI overpasses the region only once.

Monitoring CO emissions of the metropolis Mexico City using TROPOMI CO observations

Tobias Borsdorff[1], Agustín García Reynoso[2], Gilberto Maldonado[2], Bertha Mar-Morales[2], Wolfgang Stremme[2], Michel Grutter[2], and Jochen Landgraf[1]

[1]Netherlands Institute for Space Research, SRON, Utrecht, the Netherlands
[2]Centro de Ciencias de la Atmósfera, Universidad Nacional Autónoma de México, México City, Mexíco

Correspondence: T. Borsdorff (t.borsdorff@sron.nl)

Abstract. The Tropospheric Monitoring Instrument (TROPOMI) on ESA Copernicus Sentinel-5 satellite (S5-P) measures ~~the~~ carbon monoxide (CO) total column ~~concentration~~ concentrations as one of its primary targets. In this study, we ~~analyse 551 TROPOMI overpasses~~ analyze TROPOMI observations over Mexico City ~~(more than 2 years of measurements) using~~ in the period 14 November 2017 to 25 August 2019 by means of collocated CO simulations ~~of~~ using the regional Weather Research and Forecasting (~~WRF) modelto~~ WRF-chem) model. We conclude on the emissions from different urban districts in the region. ~~The WRF simulation distinguishes the~~ Our WRF-chem simulation distinguishes CO emissions from the districts Tula, Pachuca, Tulancingo, Toluca, Cuernavaca, Cuautla, Tlaxcala, Puebla, ~~the metropolian area of MexicoCity (CDMX), and the adjoint urban area (ACDMX, CDMX surrounding municipalities from estate of Mexico)~~ Ciudad de Mexico, and Arena Ciudad de Mexico by 10 separate tracers. ~~Using a regularised~~ For the data interpretation, we apply a source inversion approach ~~, the TROPOMI observations yields 0.10 Tg/yr and 0.08 Tg/yr CO emissions from the Tula and Pachuca urban areas in the North of Mexico city. This exceeds significantly~~ determining per district the mean emission and the temporal variability, latter regularized to reduce the propagation of the instrument noise and forward model errors in the inversion. In this way, the TROPOMI observations are used to evaluate the "Inventario Nacional de Emisiones de Contaminantes Criterio" (INEM) inventory that was adapted to the period 2017-2019 ~~and results in an~~ using in-situ ground-based observations. For the Tula and Pachuca urban areas in the North of Mexico City, we obtain 0.10 ± 0.004 Tg/yr and 0.09 ± 0.005 Tg/yr CO emissions, which exceeds significantly the INEM emissions <0.008 Tg/yr for both areas. ~~For CDMX~~On the other hand for Ciudad de Mexico, TROPOMI estimates emissions of 0.14 ± 0.006 Tg/yr CO, which is about half of the INEM emissions of 0.25 Tg/yr ~~. ACDMX area, however, has a higher emissions with 0.29~~ and for the adjacent district Arena Ciudad de Mexico the emission is 0.28 ± 0.01 Tg/yr according to TROPOMI observations versus 0.14 Tg/yr as stated by the INEM inventory. ~~The~~ Interestingly, the total emission of both districts is similar (~~0.43~~ 0.42 ± 0.016 Tg/yr TROPOMI versus 0.39 Tg/yr adapted INEM emissions). Moreover, for both areas we found that the TROPOMI emission estimates ~~for CDMX and ACDMX~~ follow a clear weakly cycle with a minimum during the weekend. This agrees well with ground-based ~~in situ~~ in-situ measurements from the "Secretaria del Medio Ambiente" (SEDEMA) and Fourier Transform Spectrometer column measurements in Mexico City that is operated by the Network for the detection of Atmospheric Composition Change Infrared Working Group (NDACC-IRWG). ~~The study shows~~ Overall, our study demonstrates an approach to ~~use~~ deploy the large amount of TROPOMI CO data to conclude on

urban emissions on sub-city scales for metropolises like Mexico City~~but also~~. Moreover, for the exploitation of TROPOMI CO observations our analysis indicates the clear need for further improvements of regional models like ~~WRF~~WRF-chem, in particular with respect to the prediction of the local wind fields.

1 Introduction

Carbon monoxide (CO) is an atmospheric trace gas emitted by incomplete combustion to the atmosphere (e.g. biomass burning, industrial activity, and traffic). Its background concentration is relatively low with an atmospheric residence time varying from days to month (Holloway et al., 2000) depending on the atmospheric concentration of the hydroxyl radical (Spivakovsky et al., 2000). These characteristics established CO as a tracer for air pollution and ~~its transport~~ transport processes in the atmosphere (e.g. (Gloudemans et al., 2009; Pommier et al., 2013; Schneising et al., 2019)).

The Tropospheric Monitoring Instrument (TROPOMI) launched 2017 as single payload of ESA's Copernicus Sentinel-5 Precursor mission aims on CO as one of its primary targets. The operational CO column product is inferred from TROPOMI's shortwave infrared measurements with daily global coverage and a high spatial resolution of 7x7 km^2 (Veefkind et al., 2012). Early in the mission, the TROPOMI CO dataset was validated with ground-based measurements of the Total Carbon Column Observing Network (TCCON) (Borsdorff et al., 2018a), and inter-compared with ~~the~~ simulated CO fields of the European Centre for Medium-Range Weather Forecasts (ECMWF) - Integrated Forecasting System (Borsdorff et al., 2018b). On 11 July 2018, it was concluded that the TROPOMI CO data quality is fully compliant with the mission requirements of 15% precision and 10% accuracy and so it was released for public usage (https://scihub.copernicus.eu).

Borsdorff et al. (2018a, 2019) illustrated the capability of TROPOMI to detect CO emissions from pollution hot spots of medium size to large cites (e.g. Yerevan, Tabriz, Urmia, and Tehran), industrial areas (e.g. Po valley in Italy), and even pollution along arterial roads in Armenia. To monitor the emissions of metropolises, data interpretation of multi-annual data sets is required. The different inversion techniques discussed by (Varon et al., 2018) for plume inversions, i.e. the source pixel method, the mass balance method and the inversion of a Gaussian plume model are appropriate to interpret emission of point sources but are less suitable for flux inversion of spatially extended sources. Therefore, in this study we estimate CO emission ~~inverting~~ by inverting simulations of the regional atmospheric modeling Weather Research and Forecasting (~~WRF~~WRF-chem) as an atmospheric tracer transport model, which allows to simulate the CO column on the spatial resolution as TROPOMI. Possible error sources of this type of flux inversion is the limited validity of the simulated wind fields, prior assumption on the spatial distribution of emissions, and the simulated atmospheric dispersion (Borsdorff et al., 2019).

Mexico City is a prime example of a CO pollution hot spot that is clearly detectable by TROPOMI. It is a ~~fast growing~~ fast-growing mega city located at an altitude of 2240 m on the Central Plateau which is surrounded by mountains. The urban area is divided in ten different urban districts (Tula, Pachuca, Tulancingo, Toluca, ~~CDMX~~CdMx, Cuernavaca, Cuautla, Tlaxcala, Puebla, ~~CDMX, and ACDMX~~Ciudad de Mexico (CdMx), and Arena Ciudad de Mexico (ACdMx)) and the metropolis has a long history of atmospheric pollution measurements. More than 29 ~~in situ~~ in-situ CO measurements stations are distributed over the city operated by the "Secretaria del Medio Ambiente" (SEDEMA, Mexican Ministry of the ~~Enviroment~~Environment).

About every ~~2~~ two years, the ministry reports on the CO emission of Mexico City. Based on the bottom-up approach using the ~~in situ~~ in-situ measurements, it is concluded that a major part of Mexico City's CO emission is caused by light duty motor vehicles ~~. SEDEMA found a decline of the CO emissions for~~ with a significant decline in the recent years. For the Zona metropolitana del valle de Mexico (ZMVM), SEDEMA reported a reduction of CO emissions from 2.04 ~~Tg/yr in 2000,~~ to 0.7 ~~Tg/yr in 2014, to~~ and 0.28 Tg/yr in the years 2000, 2014, and 2016 ~~SMA-GDF (2018). Here the emission estimation changed by 0.42 Tg/yr in only 2 years from 2014 to 2016, due to a change in the mobile emission model from 'mobile' to 'moves'. The emission estimate for the total central area wich is 0.73 Tg/yr for the year 2016 splits up into 0.28 Tg/yr for CDMX, 0.43 Tg/yr for ACDMX, and 0.02 Tg/yr for Tizayuca~~SMA-GDF (2018).

~~Moreover,~~

These in-situ measurements are complemented by ground-based ~~FTIR measurements are regularly performed as part~~ FTIR observations of the NDACC (Network for the detection of Atmospheric Composition Change) - IRWG (Infrared Working Group) ~~, which provide~~ network, which among other products provide regularly CO total column concentrations. Using ~~these measurements~~ NDACC and IASI satellite observations of CO, Stremme et al. (2013) estimated the overall annual CO emission of Mexico City to be about 2.15 Tg/yr for the year 2008. Building on this, TROPOMI CO observations add new possibilities for air quality monitoring due to the regional coverage, the daily overpass combined with the high precision of the data.

In this study, we ~~analyse more than 2~~ analyze about two years of TROPOMI CO measurements using collocated ~~WRF~~ WRF-chem CO simulations for Mexico to get more insight into the emission of Mexico City. To this end, in Section 1 ~~introduces~~ we introduce the TROPOMI CO dataset and the simulation of the ~~WRF model .~~ WRF-chem model and Section 2 describes our methodology to fit the ~~WRF~~ WRF-chem model to the TROPOMI data for emission estimates. Sections 3 discusses our finding and section 4 gives the summary and conclusion.

2 TROPOMI CO data set

~~This study uses~~

To investigate CO emission of the Mexico City metropolis, we select the TROPOMI dataset of CO total column ~~concentration between 14th~~ observations between 14 November 2017 and ~~25th~~ 25 August 2019 over Mexico. ~~On 5 August, 2019, the spatial sampling of the data product at satellite nadir geometry was improved from 7x7 km^2 to 7x5.6 km^2 due to a shorter readout time of the detectors. The data processing deploys~~ The data are processed with the shortwave infrared CO retrieval (SICOR) algorithm that was developed for the Copernicus operational data processing (Landgraf et al., 2016a). Algorithm settings like the spectral windows, priori profiles and ~~auxiliary are introduced in (Landgraf et al., 2016b). The retrieval utilizes an forward calculation accounting~~ other auxiliary data are reported by Landgraf et al. (2016b). The SICOR algorithm accounts for for atmospheric scattering ~~that allows to retrieve~~ by retrieving effective cloud parameters (altitude, optical thickness) together with the total column concentrations of CO and of the interfering gases ~~H_2O, HDO and CH_4 (Vidot et al., 2012). The forward calculation~~ H_2O, HDO and CH_4. The radiative transfer simulation uses the HITRAN 2016 database for all species as described by ~~(Borsdorff et al., 2019)~~ Borsdorff et al. (2019) and the inversion deploys the profile scaling approach that scales a reference profile to fit the spectral measurement (Borsdorff et al., 2014). Here, the priori profile is taken from a spatio-temporally resolved atmospheric transport simulations of the TM5 model (Krol et al., 2005). The TROPOMI ~~data product also provides~~ CO data product includes the total column averaging kernel ~~a_{col}~~ a_{col} that relates the ~~real~~ true vertical CO profile ~~ρ_{true}~~ ρ_{true} to the retrieved total column concentration ~~c_{ret}~~ c_{ret} following the equation

$$c_{\cancel{ret}\,\mathrm{ret}} = \cancel{a_{col}\rho_{true}}\, a_{\mathrm{col}}\rho_{\mathrm{true}} + \epsilon \tag{1}$$

with the noise contribution ϵ. ~~In this study we limit our~~ This study limits the analysis to scenes under clear-sky and low-cloud atmospheric conditions~~, which corresponds to the filtering of~~. This corresponds to quality assurance value $q > 0.5$ ~~. Individual~~ which is also provided by the S5P data product. Finally, the individual TROPOMI CO orbits show an artificial striping in flight direction, probably due to ~~calibration inaccuracies. For de-striping~~a deficient instrument calibration. To reduce this feature, we apply an a posteriori ~~correction to the retrieved CO columns as discussed in~~ data correction as discussed by (Borsdorff et al., 2019) based on frequency filtering in the Fourier space. Finally, on 5 August, 2019, the spatial sampling of the data product at satellite nadir geometry was improved from 7x7 km^2 to 7x5.6 km^2 due to a shorter readout time of the detectors. This event is covered by our data set.

3 Methodology

3.1 The ~~WRF~~ WRF-chem model

We simulate the TROPOMI CO column concentrations ~~measured by TROPOMI~~ by deploying the ~~WRF-Chem~~ WRF-chem model version 3.9.1.1. The simulation covers the time period of TROPOMI measurements on the regional domain shown in Fig. 1. ~~It assumes a time invariant CO background concentration and does not account for atmospheric chemistry (Dekker et al., 2017)~~ We ignore photo-chemical oxidation and secondary production of CO in the atmosphere (chem_opt option 106 (RADM2-KPP), as a tracer with gaschem off), which is justified by the long lifetime of CO compared with the size of the model domain as discussed by Dekker et al. (2017). Especially, for the region of Mexico City the contribution of atmospheric chemistry to the total CO concentration is less than 3% as presented by Mejia (2020). Hence, WRF-chem simulates the transport of CO surface emission as traces as done by e.g. Borsdorff et al. (2019); Dekker et al. (2017, 2018). The spatial resolution of the simulation is chosen to be comparable with the TROPOMI CO product sampling. Each grid cell of the considered simulation domain (~~270x270km~~270x270 km^2) is ~~3x3k~~3x3 km^2. The ~~WRF~~ WRF-chem simulation employs the emission inventory “Inventario Nacional de Emisiones de Contaminantes Criterio” (INEM) for the year 2013 but scaled by a factor of 0.48 to make it applicable ~~for~~ to the years 2017 to 2019. ~~This factor was obtained when comparing the model results against~~ Here the scaling factor is based on recent SEDEMA surface measurements (García-Reynoso et al., 2018). The inventory ~~is time dependent and accounts for the~~ includes diurnal, week-to-week and monthly variations of the ~~emissions. Moreover~~CO emissions, where weekly and daily temporal profiles are derived from traffic counts in Mexico. The inventory is described in more detail by (García-Reynoso et al., 2018). Finally, the model run is constraint by NCEP North American Mesoscale (NAM) 12 km analysis wind fields (NCEP, 2015) ~~. Finally, WRF~~ and yields vertical CO concentration profiles for every latitude/longitude grid cell and every model time step and tracer run. ~~To estimate different CO emissions areas in central Mexico, the WRF~~

The WRF-chem simulation uses ten independent ~~tracer, one for~~ tracers to estimate the CO emissions of the areas Tula, Pachuca, Tulancingo, Toluca, Cuernavaca, Cuautla, Tlaxcala, Puebla, the metropolian area of Mexico City ~~(CDMX)~~CdMx, and the adjoint urban area ~~(ACDMX). Hence, the~~ ACdMx. The total simulated CO field is given by the sum of the simulated CO fields of the tracer~~together with the spatiotemporal constant CO background~~. Since no atmospheric chemistry is accounted, ~~the~~ each CO tracer field is linear in a ~~sealing α_i of~~ the corresponding emissions per district,

$$\cancel{\mathbf{F}_{\mathrm{WRF}}}\mathbf{F}_{\mathrm{WRF}}(\alpha_1,\cdots,\alpha_{10}\cancel{,\alpha_{\mathrm{bg}}}) = \sum_{i=1}\cancel{^{10}\mathbf{k}}^{10}\mathbf{k}_i\alpha_i\cancel{+\mathbf{k}_{\mathrm{bg}}\alpha_{\mathrm{bg}}} \tag{2}$$

where ~~$\mathbf{k}_i$~~ α_i is the corresponding scaling factor and $\mathbf{k}_i$ represents the CO tracer field for the reference emission (adapted INEM data) for $\alpha_i = 1$. ~~Further, the forward model assumes linear dependence of CO background field $\mathbf{k}_{\mathrm{bg}}$ with scaling parameter α_{bg} (Borsdorff et al., 2019).~~

Before ~~contrasting the model simulations with the observations, we first~~ using our model to simulate TROPOMI data, we interpolate the model fields to the geolocation and time of the TROPOMI observations~~and second~~. Subsequently, we integrate the model CO profiles to total column densities by applying the total column averaging kernel of the TROPOMI CO retrieval following equation 1. We summarize this numerical step in the observation operator $\mathcal{O}$, which transforms the forward model into

$$\cancel{\mathbf{F}_{\mathrm{sat}}}\mathbf{F}_{\mathrm{sat}}(\alpha_1,\cdots,\alpha_{10}\cancel{,\alpha_{\mathrm{bg}}}) = \sum_{i=1}^{10}\mathcal{O}(\cancel{\mathbf{k}}\mathbf{k}_i)\alpha_i\cancel{+\mathbf{k}_{\mathrm{bg}}\alpha_{\mathrm{bg}}} \tag{3}$$

Hence, the operator $\mathcal{O}$ accounts for the TROPOMI specific vertical sensitivity, which can change from measurement to measurement and so ensures that the comparison between TROPOMI and ~~WRF~~ WRF-chem is free of the null-space or smoothing error (Rodgers, 2000; Borsdorff et al., 2014). Here, the scaling factors α_i ~~per emission area~~ are not affected by the operation.

In a next step, we transform Eq. (3) to

$$\cancel{\mathbf{F}_{\mathrm{sat}}}\mathbf{F}_{\mathrm{sat}}(E_1,\cdots,E_{10}\cancel{,\alpha_{\mathrm{bg}}}) = \sum_{i=1}^{10}\mathcal{O}(\tilde{\mathbf{k}}_i)E_i\cancel{+\mathbf{k}_{\mathrm{bg}}\alpha_{\mathrm{bg}}} \tag{4}$$

~~Here, $\tilde{\mathbf{k}}_i = \frac{\mathbf{k}_i}{E_{i,INEM}}$ and $E_i = \alpha_i E_{i,INEM}$~~ where $\tilde{\mathbf{k}}_i = \frac{\mathbf{k}_i}{E_{i,INEM}}$ and $E_i = \alpha_i E_{i,INEM}$ with the corresponding emissions ~~$E_{i,INEM}$~~ $E_{i,INEM}$ of the INEM inventory interpolated to the TROPOMI overpass time. ~~)~~

~~Finally, to~~ To improve the capability of ~~the~~ our forward model to fit TROPOMI observations, we ~~induce a linear altitude dependence of the simulated CO column $\mathbf{k}_{\mathrm{elv}} = z - z_{\mathrm{ref}}$~~introduce a spatially constant CO background field $\mathbf{k}_{\mathrm{bg}}$ and an altitude dependence term $\mathbf{k}_{\mathrm{elv}} = z - z_{\mathrm{ref}}$ with corresponding scaling factors α_{bg} and α_{elv}. Here, z is the ~~mean elevation in~~ respective elevation of the TROPOMI CO ground pixels and ~~$z_{\mathrm{ref}} = 2240$ m the reference altitude which is~~ $z_{\mathrm{ref}} = 2240$ m is an arbitrary reference altitude set to the elevation of Mexico City~~.~~,

$$\cancel{\mathbf{F}_{\mathrm{sat}}}\mathbf{F}_{\mathrm{sat}}(E_1,\cdots,E_{10},\alpha_{\mathrm{bg}},\alpha_{\mathrm{elv}}) = \sum_{i=1}^{10}\mathcal{O}(\tilde{\mathbf{k}}_i)E_i + \cancel{\mathbf{k}}\mathbf{k}_{\cancel{\mathrm{bg}}\mathrm{bg}}\alpha_{\cancel{\mathrm{bg}}\mathrm{bg}} + \cancel{\mathbf{k}}\mathbf{k}_{\cancel{\mathrm{elv}}\mathrm{elv}}\alpha_{\cancel{\mathrm{elv}}\mathrm{elv}}. \tag{5}$$

~~With this additional degrees of freedom the forward model can~~ These two effective model components account for CO contribution over the Mexico City area originating from outside the model domain such as fires, power plants, biogenic production, other cities as well as the long range transport (Borsdorff et al., 2019) and an altitude dependent linear vertical gradient of the CO columns. Both do not interfere with any localized emission sources. They mitigate shortcomings of the ~~WRF simulations using a spatially constant CO background~~WRF-chem simulations ignoring CO boundary conditions at the model domain.

~~In our simulation of TROPOMI CO observations, we assume that the local enhancements of CO are due to emissions of the city districts of the same day, whereas emissions from outside the domain as well as~~ Finally, for the interpretation of our CO forward simulations, we make an important assumption. Although the WRF simulations account for the temporal accumulation of ~~CO emission of the domain is described by the background CO field. Therefore, it means that the inferred emissions E_i represents an emission estimate~~ the localized CO emission over days and weeks, we allocate an emission estimate of the corresponding overpass time to each TROPOMI overpass. Here, we assume that a TROPOMI CO image is dominated by the emissions of the urban ~~district~~ districts for the particular observation day~~. Moreover, the effective model parameter α_{bg} and α_{elv} may vary between different TROPOMI overpasses~~, where the temporal accumulation of CO from previous days is partly described by the WRF simulation due to the corresponding scaling of the inventory and partly mitigated by fitting the nuisance parameter α_{bg} and α_{elv}.

3.2 Inversion methodology

Interpreting a series of n TROPOMI CO images

$$y = (y_1, \cdots, y_n) \tag{6}$$

at overpass times $t_0, \cdots, t_n$ means to estimate the corresponding emissions given by the state vector

$$x = (x_1, \cdots, x_n)\,, \tag{7}$$

where each element comprises

$$x_i = (E_{1,i}, \cdots, E_{10,i}, \alpha_{\mathrm{bg},i}, \alpha_{\mathrm{elv},i}) \tag{8}$$

at the corresponding time t_i. Our linear forward model in Eq. (5) describes the measurement vector y by

$$\begin{pmatrix} y_1 \\ y_2 \\ \vdots \\ y_n \end{pmatrix} = \begin{pmatrix} \mathbf{K}_1 & 0 & \cdots & 0 \\ 0 & \mathbf{K}_2 & \cdots & 0 \\ \vdots & \vdots & \ddots & \vdots \\ 0 & 0 & \cdots & \mathbf{K}_n \end{pmatrix} \begin{pmatrix} x_1 \\ x_2 \\ \vdots \\ x_n \end{pmatrix} \tag{9}$$

with the forward model Jacobian $\mathbf{K}_i = (\mathcal{O}(\tilde{\mathbf{k}}_{1,i}), \cdots \mathcal{O}(\tilde{\mathbf{k}}_{10,i}), \mathbf{k}_{\mathrm{bg},i}, \mathbf{k}_{\mathrm{elv},i})$, in short $y = \mathbf{K}x$. Equation (9) can be inverted by

$$x_{\mathrm{est}} = \min_x \left\{ ||y - \mathbf{K}x||^2_{\mathbf{S}_e} \right\}\,, \tag{10}$$

which is equivalent to the solution $(x_{\text{est},1},\cdots,x_{\text{est},n})$ of the individual problems $y_i = \mathbf{K}_i x_i$ due to the block diagonal form of Eq. (9). Here, the norm of an arbitrary vector p is defined by $||p||^2_{\mathbf{S}_\text{e}} = p^T\mathbf{S}_\text{e}^{-1}p$ and $\mathbf{S}_\text{e}$ is the measurement error covariance matrix with the variance of the TROPOMI retrieval error on the diagonal.

Due to measurement noise and forward model errors, the least squares inversion of Eq. (10) results in unfavorable error propagation and so requires regularization. Because our problem is linear in the state vector x regularization can be performed as part of the fitting approach or a posteriori to the least squares solution, without loss of generality. To regularize the noise propagation, we first derive the temporal mean

$$\bar{x}_\text{est} = \frac{1}{n}\sum_{i=1}^{n} x_{\text{est},i} \tag{11}$$

from the non-regularized solution in Eq. (10). This modifies our cost function to

$$x_\text{est} = \min_x \left\{ ||y-\mathbf{K}x||^2_{\mathbf{S}_\text{e}} \right\} \quad \text{with} \quad \bar{x} = \frac{1}{n}\sum_{i=1}^{n} x_i \tag{12}$$

In this way, we divided the solution of the original inversion problem (10) in two steps: First we determine the mean emission from the individual least squares solutions $x_{\text{est},i}$, which yields the constrained least squares problem in Eq. (12) to describe the temporal variability. The side constraint guarantees that measurement information is not used twice. Finally, we add an additional Tikhonov side constraint to Eq. 12 to regularize the error propagation,

$$x_\text{est} = \min_x \left\{ ||y-\mathbf{K}x||^2_{\mathbf{S}_\text{e}} + ||x-\bar{x}||^2_{\mathbf{\Gamma}} \right\} \tag{13}$$

with

$$\bar{x} = \frac{1}{n}\sum_{i=1}^{n} x_i \,. \tag{14}$$

Here, $\mathbf{\Gamma}$ is an appropriate regularization matrix. For a block diagonal form of $\mathbf{\Gamma}$ analogous to the Jacobian in Eq. (9), namely

$$\mathbf{\Gamma} = \begin{pmatrix} \mathbf{\Gamma}_1 & 0 & \cdots & 0 \\ 0 & \mathbf{\Gamma}_2 & \cdots & 0 \\ \vdots & \vdots & \ddots & \vdots \\ 0 & 0 & \cdots & \mathbf{\Gamma}_n \end{pmatrix} \tag{15}$$

the minimization problem (13) decomposes into n problems

$$x_\text{est,i} = \min_{x_i} \left\{ ||y_i-\mathbf{K_i}x_i||^2_{\mathbf{S}_\text{e}} + ||x_i-\bar{x}||^2_{\mathbf{\Gamma}} \right\} \tag{16}$$

which are only coupled by the external side constraint (14). A closer look at our inversion problem shows that the two constraints have similar effects. The Tikhonov constraint $||x-\bar{x}||_{\mathbf{S}_\text{e}}$ minimizes the variation of the state vector around its mean depending on the regularization parameter λ, whereas the external constraint requires strict conservation of the mean.

Therefore, in practice, we solve the inversion (16) and evaluate the external constraint on the mean afterwards to confirm proper use of the measurement information. Its solution is given by

$$x_{\mathrm{est,i}} = \mathbf{G}_{\mathrm{i}}(y_i - \mathbf{K}_i \bar{x}_i) + \bar{x}_i \tag{17}$$

with the gain matrix

$$\mathbf{G}_i = (\mathbf{K}_i^T \mathbf{S}_{\mathrm{e,i}}^{-1} \mathbf{K}_i + \mathbf{\Gamma}_i)^{-1} \mathbf{K}_i^T \mathbf{S}_{\mathrm{e,i}}^{-1} \tag{18}$$

The inversion's averaging kernel relates the 'true' state vector $x_{\mathrm{true},i}$ to $x_{\mathrm{est},i}$, namely

$$x_{\mathrm{est},i} = \mathbf{A}_i \left(x_{\mathrm{true},i} - x_i\right) + \bar{x} \tag{19}$$

with

$$\mathbf{A}_i = \mathbf{G}_i \mathbf{K}_i \tag{20}$$

$\mathbf{A}_i$ represents the derivative $\mathbf{A}_{\mathrm{i,kl}} = \frac{\partial x_{\mathrm{est},j}}{\partial x_{\mathrm{true},l}}$, where its diagonal elements describe the retrieval sensitivity of a state vector element to its true value. The degree of freedom for signal

$$\mathrm{DFS}_i = \mathrm{trace}(\mathbf{A}_i)\ , \tag{21}$$

indicates the total number of independent pieces of information.

To evaluate the fit quality for each overpass, we consider the fit residuals $\delta_i = y_i - \mathbf{K}_i x_{\mathrm{est},i}$. Additionally, we evaluate the goodness of the fit described by the reduced chi squared value,

$$\chi_i^2 = \frac{1}{\nu_i} \sum_{l=1}^{L} (\delta_i, l / y_{\mathrm{err},ik})^2\ . \tag{22}$$

Here L is the number of observation of a single overpass, $y_{\mathrm{err},i}$ the retrieval error, and $\nu_i = L - \mathrm{DFS}_i$.

3.3 ~~Pre-fit~~Estimate of the mean emissions

~~In a pre-fit step we~~ The first step of the inversion described in the previous section means to determine the prior emissions from a set of TROPOMI data with highest information content ~~, such that the emissions can be inferred without any regularization, $\Gamma = 0$~~using a non-regularized least squares fit, $\mathbf{\Gamma} = 0$. Here, the individual emission estimates may be noisy due to ~~non-optimized noise~~ enhanced error propagation in the inversion, however, averaging all inversions reduces noise contribution and so gives a reliable estimate of a mean emission for the different districts. The validity of this approach ~~depends crucially~~ highly depends on the selected data set of TROPOMI overpasses. On the one hand, ~~it~~ the ensemble should be large enough to estimate mean emissions for the ~~period of TROPOMI observations, and~~ considered time period, but on the other hand ~~strict data filtering is required to get~~ it should be strictly filtered for cases where the forward model is in good agreement with the measurement such that a stable inversion ~~with little forward model errors.~~

of the all emissions is possible. The information content of a single overpass varies and depends on several aspects: (1) The number of useful measurements and their cloud coverage changes between different TROPOMI overpasses. Here, clouds shield the lower troposphere, where atmospheric measurements are particular sensitive to the surface emissions E_i. (2) The pixel size at the swath edge is about 32 km and so about 5 times larger than at the sub-satellite point. This reduces not only the number of pixels covering a certain area but also the sensitivity of the individual TROPOMI observations. (3) The quality of the forward model depends on the meteorological situation, where we consider model simulations for low wind speeds more reliable. ~~This~~ These considerations led to the criteria of the data filtering ~~for the pre-fit. Thus, we~~ to determine the mean emission for each district. We only select overpasses which meet ~~all of following~~ both filter criteria:

- 70 % of the data domain is covered by TROPOMI observations
- for all observations the across track pixel size is < 15 km.
- ~~the average wind speed of the scene is < 4 m/s.~~
- ~~The fit residuum $\langle\delta\rangle < 8$ppb, and the standard deviation $\sigma(\delta) < 8$ppb to limit the effect of too large forward model errors.~~
- ~~$\sigma(\delta)/\delta(\mathbf{y}_{\mathrm{meas}}) < 0.65$ to ensure that the forward model can explain the variability of the measured CO field.~~
- ~~$\sigma(\mathbf{F}(\mathbf{x})) > 4$ ppb to ensure that the model data contain a clear pollution signatures.~~
- ~~the Pearson correlation coefficient $r > 0.3$ between $CO_{TROPOMI}$ and CO_{WRF}.~~

The filter criteria reduce the original set of 551 overpasses to ~~148~~199, which we consider to be sufficient to estimate the overall average emission rate per district, yielding ~~the prior state vector $\mathbf{x}_a$~~ $\bar{x}$. For this we use the median instead of the mean because of its robustness against outliers. With the same reasoning we define the percentile difference

$$\delta P_j = \left|\frac{P_j(84.1) - P_j(15.9)}{2}\right| \tag{23}$$

, to describe scattering in the data, which corresponds to the standard deviation of normal distributed parameters. Finally, we calculate the error of the mean using the percentile difference.

3.4 ~~Final-fit~~Final data product

Subsequently, the final data reduction ~~steps is performed . To reduce the noise propagation in the inversion and to become independent on the prior data selection, we regularize the inversion to the prior state determined by the pre-fit. Here~~step is performed solving the inversion problem (13). For all overpasses, we choose ~~Γ~~ $\boldsymbol{\Gamma}_i$ to be a diagonal matrix with

$$\cancel{diag\Gamma}\,\mathrm{diag}\,\boldsymbol{\Gamma}_i = [\gamma_1, \gamma_2, \cdots, \gamma_{10}, 0, 0] \tag{24}$$

~~such~~ where the zeros ensure that the elements of the state vector ~~α_{bg} and α_{elv}~~ α_{bg} and α_{elv} are not regularized. Obviously, the regularization parameter ~~γ_i~~ γ_k must be well-chosen to optimize the balance between minimum error propagation on the fit parameter and maximum information content inferred from the measurement. If ~~γ_i~~ γ_k is chosen too small, the propagation of the TROPOMI measurement noise as well as retrieval biases and forward model errors dominates the inversion. If ~~γ_i~~ γ_k is chosen too large, the estimated state vector reproduces the prior estimate without appropriate use the information content of the measurement. For our application, we fix the regularization parameter ~~γ_i for $i = 1, \cdots, 10$~~ γ_k for $k = 1, \cdots, 10$ to constant values such that the scatter of the retrieved emissions stays within predefined boundaries.

Considering the temporal variation of the INEM emissions to be about 40%, we adjusted the regularization parameter $\gamma_1, \cdots, \gamma_{10}$ such that the retrieved emissions vary ~~with~~ within 60% around their average. ~~This~~ The value 60% is empirical chosen to balance information content against noise propagation. It puts a moderate constraints on the inversion ensuring on the one hand a stable inversion and on the other hand a realistic variation of the retrieved emissions around the priori.

~~A~~ One great advantage of the ~~Final-fit compared to the Pre-fit is that the retrieved emissions can be filtered~~ final retrieval product is that it includes the averaging kernel $\mathbf{A}_i$. This can be used to filter the data with respect to the information provided by the TROPOMI measurements. ~~We~~ For each tracer emission, we filter on the ~~information for each tracer emission E_i individually, considering inferred emissions with $(AK(i,i) > 0.3)$~~individual emission E_l, considering averaging kernel values $\mathbf{A}_{l,l} > 0.3$. This form of data mining optimizes the data use, keeping in mind that TROPOMI overpasses may be appropriate to determine one specific source but not all sources simultaneously. ~~In this manner, noise propagation in the inversion can be minimized. This~~ The concept of information content based filtering turned out to be very useful ~~. The filter criteria of the Pre-fit are not required anymore for the Final-fit to achieve a very similar performance. A filtering like this is not possible for the Pre-fit since the averaging kernel of an regularized retrieval is by definition $(AK(i,i) = 1)$~~and enhances the data exploitation compared to the non-regularized least squares fitting used to determine the mean emission values.

4 Results

Fig. 2 shows the ~~fitted CO background~~ CO background that was fitted as an auxiliary parameter during the inversion described in Sec. 3.2. The concentration and its annual cycle are shown. Here, the biomass burning season between February and June causes the corresponding CO enhancement, whereas lower CO concentrations are observed during the ~~rain~~ rainy season between June and November. The extremely high CO column values on the 15th May 2019 are due to the transport of CO enriched air from wild fires in the South-West of Mexico in to the model domain. Figure 3 shows the CO concentration in the state of Mexico under normal conditions and after the fires, which caused a serious health hazard in Mexico City. These type of fires outside the model domain create an inhomogeneous background CO field over Mexico City, which cannot be described by our forward model. Only fitting a ~~scaling to a constant background field~~ constant background is not sufficient in ~~this~~ these extreme cases and so during the fire season many data cannot be ~~considered~~used (we excluded the month May and June 2019).

Figure 4 shows three examples of TROPOMI overpasses, which includes a pixel resolution of 7x7 km^2 (panel (a), (b), and (c)) and the enhanced spatial resolution of 7x5.6 km^2 (panel (d)), where latter is the TROPOMI instrument baseline since the 6th of August 2019. Focusing on the dry season, the TROPOMI instrument can detect distinct CO enhancements over the different emission areas in Central Mexico with the retrievals from single orbit overpasses (see left column of Fig. 4). After fitting our forward model to the TROPOMI measurements ~~, as part of the Final-fit,~~ brings simulated data and observations into good agreement as illustrated in Fig. 4. Particular for low wind speed conditions in Fig. 4(a), TROPOMI and ~~WRF~~ WRF-chem show distinct CO enhancements over the different emission areas of Mexico. Furthermore, the transport of CO enhanced air form Mexico City towards the South following the mountain orography and the accumulation of CO in the South is seen by TROPOMI in agreement with the ~~WRF~~ WRF-chem simulation (4(c). This clearly shows that regional models like ~~WRF~~ WRF-chem have a great potential ~~for the interpretation and analysis of TROPOMI data~~to reproduce the large-scale patterns seen by the TROPOMI instrument. However, we also found clear localized residuals in the difference δ_j between observations and forward model. (right column of Fig. 4). For atmospheric conditions under high wind speeds the ~~WRF~~ WRF-chem simulations can deviate more from the TROPOMI measurements as shown in Fig. 4 (c). Here, the plume of CO enriched air extending from Mexico City towards the North is simulated very narrow compared to the more dispersed plume seen by TROPOMI. This points to ~~an~~ a possible underestimation of the atmospheric dispersion in the ~~WRF~~ WRF-chem simulation. A very prominent residual between TROPOMI and ~~WRF~~ WRF-chem is shown in 4 (d) but also present in 4 (a) and (b). Here TROPOMI measures a strong CO enhancement in the North of Mexico City that is not reproduced by the ~~WRF~~ WRF-chem model. This points at a deficient spatial distribution of INEM emissions.

For each tracer domain Fig. 5 (a) shows ~~for each tracer doamin the averaged~~ the mean emissions of the ~~Final-fit derived from the TROPOMI data E_i in comparison to the ones of the Pre-Fit and the priori emission used for the WRF simulation (adapted INEM inventory). We~~ the adapted INEM inventory, the non-regularized least squares fit and the final data product. The mean emissions agree very well between the last two approaches, indicating that the final inversion in Eq. 17 satisfies the constraint of the pre-defined mean value. This supports our assumption that the external constraint does not have to be accounted for the chosen Tikhonov constraint of the inversion. The scatter of the least squares product is high and in most cases exceeds 100% (see Fig. 5 (b)), which is expected for the non-constraint inversion. Moreover, we find significant differences between the emissions of the ~~priori and the Final-fit~~prior and the final data product. The retrieved emissions ~~of the Final-fit from~~ for the urban districts Tula (0.10 $\pm$ 0.004 Tg/yr) and Pachuca (~~0.08~~ 0.09 $\pm$ 0.005 Tg/yr) in the North of Mexico ~~city~~ City seem to be underestimated by the emission inventory (both were less then 0.008 Tg/yr). ~~Furthermore~~ It is not yet clear what sources are missing in the inventory, this needs to be addressed in future studies. However, we identified an oil refinery and a power plant near to Tula and cement and lime kilns near to Pachuca that could contribute to the CO emissions. Furthermore, we found that the emission of the central part of Mexico ~~city (CDMX~~City (CdMx) is assumed too high in the ~~priori emissions~~ adapted INEM inventory (0.25 Tg/yr)~~. The~~ , where TROPOMI measurements indicate lower values for ~~CDMX~~ CdMx (0.14 $\pm$ 0.006 Tg/yr)~~which come~~ . This comes along with higher values for the ~~district ACDMX (0.29~~ adjacent district ACdMx (0.28 $\pm$ 0.01 Tg/yr). The sum of both emissions (~~0.43~~ 0.42 $\pm$ 0.016 Tg/yr) is similar to the priori emissions (0.39 Tg/yr). This may mean that the total emissions of the domain including ~~CDMX and ACDMX~~ CdMx and ACdMx is well represented in the emission inventory but only the spatial distribution of the source intensity ~~is unrealistic~~needs refinement.

~~In General, the retrieved emissions of the Final-fit are in good agreement with the one of the Pre-fit. The explanation for this is simple, the retrieved emission of the Pre-fit are used as priori for the regularized inversion of~~ The χ^2 values in Fig 5 clearly show that the agreement between TROPOMI and WRF can be improved by fitting the emissions of the different city districts (blue line) instead of using the INEM inventory (grey line). The regularization approach increases the χ^2 values (green bars) because the inversion can less compensate differences between TROPOMI and WRF by choosing unrealistic emissions. However, the ~~Final-fit as described in Sec 3.4. The scatter of the individual retrievals of the Pre-fit is high and in most cases exceeds 100% (see Fig. 5 (b)) . This is most probably caused by forward model errors as discussed before. Furthermore, non-uniform variation of the background CO concentration can be a additional reason for this scatter (as shown in Fig. 3). However, the average of the individual retrievals of the Pre-fit is more trustworthy (see error bars in Fig. 5 (a)) and by that is our best estimate of an unbiased emission priori for the Final fit. The regularization of the~~ χ^2 values of the Final-Fit ~~succeeds to reduce the scatter of the individual retrieval~~ are still lower than the ones for the prior INEM emissions (grey line). Overall, the χ^2 values exceeds 1 which indicates that the difference between TROPOMI and WRF is dominated by systematic errors in the WRF simulation.

For a correct interpretation of the retrieved emissions the averaging kernel, as shown in ~~5 (b)).~~

~~In~~ Fig. 6 ~~, the averaging kernel of the examples cases shows~~ for four example cases, offers several advantages. The figure shows that generally the averaging kernels have high values on the diagonal indicating ~~that the Final-fit even using the regularization can~~ high sensitivity to the quantity to be retrieved. It indicates that TROPOMI measurements can be used to distinguish emissions of the different urban districts of Mexico~~. Moreover, the averaging kernel shows that the Final-fit inversion is insensitive to deviations of the Tulancingo emission from the prior estimate. Whereas the Pre-fit inversion estimates very small emissions for this district, the subsequent regularization changes the emission only marginally~~, with the exception of the emissions of district Tulancingo. Due to the small mean emission, the averaging kernel indicates a low sensitive of the data product. Furthermore, the ~~regularization of the Final-fit imposes~~ averaging kernel shows cross-correlations between the different elements of the state vector due to the regularization. Although these interdependencies exist, e.g. between ~~CDMX and ACDMX as can be seen~~ the emission of CdMx and ACdMx as shown in panel (d) of Fig. 6, ~~which~~ these are still small compared the diagonal. ~~In general, for a correct interpretation of the retrieved emissions the averaging kernels shown in Fig. 6 needs to be taken in account when ever possible. So, one can~~ The averaging kernel information is very useful to filter the emission product with respect to the information provided by the TROPOMI measurements. ~~Hence, for the Final-fit, we filter on the information for each tracer emission E_i individually. This~~ Using the sensitivity of individual sources, this results in different number of coincidences for the different districts (panel (c) of Fig 5). This form of data mining optimizes the data use, keeping in mind that TROPOMI overpasses may be appropriate to determine one specific source but not all sources simultaneously. In this manner, ~~noise~~ error propagation in the inversion can be minimized.

Due to the ~~reduced~~ little scatter and the higher data amount of the ~~Final-fit~~ final data product for the suburbs ~~CDMX and ACDMX, the Final-fit~~ CdMx and ACdMx allows to conclude on the time dependent variability of emission~~in Mexico City~~. Figure 7 (a) shows the time series of the emission for ~~CDMX and ACDMX~~CdMx and ACdMx, which vary around the priori value. This temporal variation is determined from the measurements as all prior information is assumed to be time invariant. The scatter of the data is still high and even includes negative values. Even though negative emissions are not physical we need to keep them in our analyses because filtering negative noise can induce a positive bias in the mean. Panel (b) of the figure shows relatively high values of the diagonal elements of the averaging kernel for the emissions of the two urban districts.

Finally, panel (c) of the figure indicates a clear weakly CO cycle in the data with low values during weekends. During the week, the CO emissions of the two districts do not differ significantly due to the error estimates and more TROPOMI data is required to further constrain the weekly cycle. We found that the CO values on Saturday and Sunday are equally low. An explanation for this could be that the main source of CO in Mexico City during the week is traffic which is responsible for the weekly cycle and the remaining sources like cooking, water heating, etc. should not change much during the weekend.

A similar weakly cycle is observed by Mexico City situ measurements provided by 29 SEDEMA ground stations. For each of the sites, we use data from 2017 to 2018 for the overpass time of TROPOMI (12h-15h local time), calculated ~~an~~ a weakly cycle and group the data in the stations located in the ~~CDMX~~ CdMx urban area and those located in the wider area of the metropolis. Figure 8a depicts the median of all weakly cycles and the standard error of the mean with a clear minimum during weekends. The error bars indicate that the overall shape of the weekly cycles for the remaining days vary a lot from station to station.

The lower CO concentrations during the weekend are also detectable with column retrievals from ground-based FTIR measurements in Mexico City 2280 m.a.s.l 19.32°N and -99.18°E at the campus of the national University by the atmospheric science center (CCA). The used spectra are recorded in the mid infrared with a resolution of 0.075 cm^{-1} (Bezanilla et al., 2014; Plaza-Medina et al., 2017) and the CO column and profile is retrieved using the standard NDACC retrieval strategy (García-Franco et al., 2018; Borsdorff et al., 2018a). Figure 8b shows the averaged weakly cycle with standard error derived from the column measurements. Due to the low data density at weekends we used the ~~full time~~ full-time range from the 5th December 2010 to the 10th September 2019 without filtering for the overpass time of TROPOMI. These independent ~~ground based~~ ground-based measurements confirm the weekly CO cycle found in the TROPOMI data.

5 Conclusions

In this study, we analyzed TROPOMI CO retrieval from 551 overpasses of the instrument over Central Mexico, which corresponds to about 2-years of measurements starting from the ~~14th~~ 14 November 2017 until the ~~25th~~ 25 August 2019. We found that urban pollution can be monitored by the TROPOMI CO data~~allows pollution monitoring by single overpasses~~. The high signal-to-noise ratio of the measurements allowed us to distinguish distinct CO enhancements over the various urban districts of Central Mexico using single orbit overpasses of TROPOMI with a high spatial resolution of 7x7 km^2 that is enhanced to 7x5.6 km^2 from the 6th of August 2019 onwards. ~~The high signal-to-noise ratio of the measurements allows to distinguish distinct CO enhancements over the various urban districts of Central Mexico using single orbit overpasses of TROPOMI.~~

With a dedicated ~~WRF~~ WRF-chem tracer simulation for the ~~full time~~ full-time range of the current TROPOMI data record, we could distinguish the contribution of ten urban districts Tula, Pachuca, Tulancingo, Toluca, Cuernavaca, Cuautla, Tlaxcala, Puebla, ~~CDMX, and ACDMX~~CdMx, and ACdMx. The model data was collocated with the TROPOMI measurements and convolved with the total column averaging kernel to account for the vertical sensitivity of the instrument. ~~The WRF~~ Here, the WRF-chem tracer simulation does not account for atmospheric chemistry and so the simulated CO tracer fields is linear in the emission rates of the different districts. The model is extended by two effective parameters describing a spatially constant CO background and a dependency of the simulated column on terrain height.

The CO emissions are determined in two steps. First, we apply a unregularized least squares fit of the model to the TROPOMI observations to determine the averaged emission per district. A strict data screening based on the measurements and ~~WRF~~ WRF-chem model simulation reduced the TROPOMI data set from 551 to ~~148 overpasses. For this data set, the fit quality is good after introducing two auxiliary fit parameters for the background variability with time and the dependency of the simulated column on terrain height. However, the individual emission rates show a high scatter exceeding 100% of the averaged emissions . When averaging the filtered emissions,~~ 199 overpasses. Second, we solve a regularized least squares problem, which minimizes the variation of the emission around its mean to reduce the noise propagation in the inversion. By means of appropriate regularization parameters, we reduce the scatter of the retrieved emissions to about 60% of the median for all urban districts. For data interpretation and screening, the use of the averaging kernel is of great advantage. The final retrieval product includes a averaging kernel as a retrieval diagnostic, which allows to analyze retrieval sensitivities and cross correlations between the inferred emission rates.

The derived averaged emissions for the various urban districts of Mexico deviates significantly from emission estimates of the "Inventario Nacional de Emissions de Contaminantes Criterio" (INEM) inventory adapted to the period 2017-2019. The TROPOMI emissions from the urban districts Tula (0.10 $\pm$ 0.004 Tg/yr) and Pachuca (~~0.08~~ 0.09 $\pm$ 0.005 Tg/yr) in the Norther of Mexico ~~city~~ City deviate significantly from the INEM inventory with 0.008 Tg/yr for both areas. For the emission of the central part of Mexico ~~city (CDMX~~City (CdMx), TROPOMI indicate 0.14 $\pm$ 0.006 Tg/yr versus 0.25 Tg/yr INEM emissions and ~~0.29~~ 0.28 $\pm$ 0.01 Tg/yr versus 0.14 Tg/yr INMEN emissions for the district ~~ACDMX~~ACdMx. Together, both districts have similar emissions with ~~0.43~~ 0.42 Tg/yr seen by TROPOMI versus 0.39 Tg/yr from the inventory, pointing to a different relative distribution of the CO emissions seen by TROPOMI.

~~Finally, in a second retrieval, we regularize the inversion towards the mean emission estimate, determined in the first step. This reduces the scatter of the retrieved emissions to about 60% of the median for all urban districts. For data interpretation and screening, the use of the averaging kernel is of great advantage. It allows to diagnose cross correlations between the inferred emission rates, which in general is weak for our application. Moreover, the~~ Moreover, using a posteriori data screening ~~uses the averaging kernel~~ to optimize data selection per emission source ~~. This filter concept is very powerful and~~ allows us to distill ~~from the data set~~ a weakly cycle of CO emission at the districts ~~CDMX and ACDMX~~ CdMx and ACdMx from the data set with a clear minimum during weekends. This finding is in agreement with ~~in situ~~ in-situ observations and ground-based FTIR measurement in the metropolis.

Our study shows the need and the potential of regional atmospheric transport modeling for the interpretation of TROPOMI CO data over metropolitan areas like Mexico City. Here, the CO pollution is a composite of emissions from different districts and its transport leads to complex CO enhancement patterns in the atmosphere. The ~~WRF~~ WRF-chem tracer model could simulate the TROPOMI measurement to a great ~~extend~~extent, however model errors are still significant and further improvement is required to fully explore the TROPOMI CO observations ~~over mega-cities~~of urban sources. Another potential error source of our method are the accuracy of the week-to-week and monthly variations of the emissions in the INEM inventory considering the fixed overpass time of TROPOMI. Furthermore, basin cities can be problematic with low wind speed for days, which could lead to accumulate signals from more than one day in the basins which is not yet covered by our approach. To account for this effect in our inversion needs major adjustments, which will be investigated in follow up studies.

6 Data availability

The TROPOMI CO data set of this study is available for download at ftp://ftp.sron.nl/open-access-data-2/TROPOMI/tropomi/co/. The ~~in situ~~ in-situ measurements in Mexico City were downloaded from http://www.aire.cdmx.gob.mx. The ground-based FTIR measurements in Mexico can be downloaded http://www.epr.atmosfera.unam.mx/ftir_data/UNAM/CO/VERTEX/v1/.

Author contributions. Tobias Borsdorff, and Jochen Landgraf performed the TROPOMI CO retrieval and data analysis. Agustin Garcia Reynoso, Gilberto Maldonado, and Bertha Mar-Morales performed the WRF-chem simulation. Wolfgang Stremme and Michel Grutter provided the ground-based FTIR measurements. All authors discussed the results and commented on the manuscript.

Competing interests. The authors declare no competing interests.

Disclaimer. The presented work has been performed in the frame of the Sentinel-5 Precursor Validation Team (S5PVT) or Level 1/Level 2 Product Working Group activities. Results are based on preliminary (not fully calibrated/validated) Sentinel-5 Precursor data that will still change. The results are based on S5P L1B version 1 data.

Acknowledgements. The presented material contains modified Copernicus data [2017,2018] The TROPOMI data processing was carried out on the Dutch national e-infrastructure with the support of the SURF Cooperative.

References

Bezanilla, A., Krüger, A., Stremme, W., and de la Mora, M. G.: Solar absorption infrared spectroscopic measurements over Mexico City: Methane enhancements, Atmósfera, 27, http://www.revistascca.unam.mx/atm/index.php/atm/article/view/43392, 2014.

Borsdorff, T., Hasekamp, O. P., Wassmann, A., and Landgraf, J.: Insights into Tikhonov regularization: application to trace gas column retrieval and the efficient calculation of total column averaging kernels, Atmospheric Measurement Techniques, 7, 523–535, https://doi.org/10.5194/amt-7-523-2014, https://doi.org/10.5194%2Famt-7-523-2014, 2014.

Borsdorff, T., aan de Brugh, J., Hu, H., Hasekamp, O., Sussmann, R., Rettinger, M., Hase, F., Gross, J., Schneider, M., Garcia, O., Stremme, W., Grutter, M., Feist, D. G., Arnold, S. G., De Mazière, M., Kumar Sha, M., Pollard, D. F., Kiel, M., Roehl, C., Wennberg, P. O., Toon, G. C., and Landgraf, J.: Mapping carbon monoxide pollution from space down to city scales with daily global coverage, Atmospheric Measurement Techniques Discussions, 2018, 1–19, https://doi.org/10.5194/amt-2018-132, https://www.atmos-meas-tech-discuss.net/amt-2018-132/, 2018a.

Borsdorff, T., de Brugh, J. A., Hu, H., Aben, I., Hasekamp, O., and Landgraf, J.: Measuring Carbon Monoxide With TROPOMI: First Results and a Comparison With ECMWF-IFS Analysis Data, Geophysical Research Letters, 45, 2826–2832, https://doi.org/10.1002/2018GL077045, https://agupubs.onlinelibrary.wiley.com/doi/abs/10.1002/2018GL077045, 2018b.

Borsdorff, T., aan de Brugh, J., Pandey, S., Hasekamp, O., Aben, I., Houweling, S., and Landgraf, J.: Carbon monoxide air pollution on sub-city scales and along arterial roads detected by the Tropospheric Monitoring Instrument, Atmospheric Chemistry and Physics, 19, 3579–3588, https://doi.org/10.5194/acp-19-3579-2019, https://www.atmos-chem-phys.net/19/3579/2019/, 2019.

Dekker, I. N., Houweling, S., Aben, I., Röckmann, T., Krol, M., Martínez-Alonso, S., Deeter, M. N., and Worden, H. M.: Quantification of CO emissions from the city of Madrid using MOPITT satellite retrievals and WRF simulations, Atmospheric Chemistry and Physics, 17, 14 675–14 694, https://doi.org/10.5194/acp-17-14675-2017, http://dx.doi.org/10.5194/acp-17-14675-2017, 2017.

Dekker, I. N., Houweling, S., Pandey, S., Krol, M., Röckmann, T., Borsdorff, T., Landgraf, J., and Aben, I.: The origin of CO sources during the 2017 high pollution episode in India determined with TROPOMI and WRF data, manuscript in prep., 2018.

García-Franco, J. L., Stremme, W., Bezanilla, A., Ruiz-Angulo, A., and Grutter, M.: Variability of the Mixed-Layer Height Over Mexico City, Boundary-Layer Meteorology, 167, 493–507, https://doi.org/10.1007/s10546-018-0334-x, https://doi.org/10.1007/s10546-018-0334-x, 2018.

García-Reynoso, J., Mar-Morales, B., and Ruiz-Suárez, L.: MODELO DE DISTRIBUCIÓN ESPACIAL, TEMPORAL Y DE ESPECIACIÓN DEL INVENTARIO DE EMISIONES DE MÉXICO (AÑO BASE 2008) PARA SU USO EN MODELIZACIÓN DE CALIDAD DEL AIRE (DiETE), Revista Internacional de Contaminación Ambiental, 34, 635–649, https://doi.org/10.20937/RICA.2018.34.04.07, https://www.revistascca.unam.mx/rica/index.php/rica/article/view/RICA.2018.34.04.07, 2018.

Gloudemans, A. M. S., de Laat, A. T. J., Schrijver, H., Aben, I., Meirink, J. F., and van der Werf, G. R.: SCIAMACHY CO over land and oceans: 2003–2007 interannual variability, Atmospheric Chemistry and Physics, 9, 3799–3813, https://doi.org/10.5194/acp-9-3799-2009, https://doi.org/10.5194%2Facp-9-3799-2009, 2009.

Holloway, T., Levy, H., and Kasibhatla, P.: Global distribution of carbon monoxide, Journal of Geophysical Research: Atmospheres, 105, 12 123–12 147, https://doi.org/10.1029/1999jd901173, https://doi.org/10.1029%2F1999jd901173, 2000.

Krol, M., Houweling, S., Bregman, B., van den Broek, M., Segers, A., van Velthoven, P., Peters, W., Dentener, F., and Bergamaschi, P.: The two-way nested global chemistry-transport zoom model TM5: algorithm and applications, Atmospheric Chemistry and Physics, 5, 417–432, https://doi.org/10.5194/acp-5-417-2005, https://www.atmos-chem-phys.net/5/417/2005/, 2005.

Landgraf, J., aan de Brugh, J., Borsdorff, T., Houweling, S., and O., H.: Algorithm Theoretical Baseline Document for Sentinel-5 Precursor: Carbon Monoxide Total Column Retrieval, Atbd, SRON, Sorbonnelaan 2, 3584 CA Utrecht, The Netherlands, 2016a.

Landgraf, J., aan de Brugh, J., Scheepmaker, R., Borsdorff, T., Hu, H., Houweling, S., Butz, A., Aben, I., and Hasekamp, O.: Carbon monoxide total column retrievals from TROPOMI shortwave infrared measurements, Atmospheric Measurement Techniques, 9, 4955–4975, https://doi.org/10.5194/amt-9-4955-2016, https://doi.org/10.5194%2Famt-9-4955-2016, 2016b.

Mejia, J. F.: Running WRF in an Atmospheric Modeling Class: challenges and learning experiences, Atmosfera, 2020.

NCEP: NCEP North American Mesoscale (NAM) 12 km Analysis, https://doi.org/10.5065/G4RC-1N91, 2015.

Plaza-Medina, E. F., Stremme, W., Bezanilla, A., Grutter, M., Schneider, M., Hase, F., and Blumenstock, T.: Ground-based remote sensing of O_3 by high- and medium-resolution FTIR spectrometers over the Mexico City basin, Atmospheric Measurement Techniques, 10, 2703–2725, https://doi.org/10.5194/amt-10-2703-2017, https://www.atmos-meas-tech.net/10/2703/2017/, 2017.

Pommier, M., McLinden, C. A., and Deeter, M.: Relative changes in CO emissions over megacities based on observations from space, Geophysical Research Letters, 40, 3766–3771, https://doi.org/10.1002/grl.50704, http://dx.doi.org/10.1002/grl.50704, 2013.

Rodgers, C. D.: Inverse methods for atmospheric sounding: theory and practice, vol. 2 of *Series on atmospheric, oceanic and planetary physics*, World Scientific, Singapore, River Edge, N.J., reprinted : 2004, 2008, 2000.

Schneising, O., Buchwitz, M., Reuter, M., Bovensmann, H., and Burrows, J. P.: Devastating Californian wildfires in November 2018 observed from space: the carbon monoxide perspective, Atmospheric Chemistry and Physics Discussions, 2019, 1–14, https://doi.org/10.5194/acp-2019-5, https://www.atmos-chem-phys-discuss.net/acp-2019-5/, 2019.

SMA-GDF: Inventario de Emisiones de la Ciudad de México 2016., Tech. rep., Secretaría del Medio Ambiente de la Ciudad de México: Dirección General de Gestión de la Calidad del Aire, Ciudad de México, 2018.

Spivakovsky, C. M., Logan, J. A., Montzka, S. A., Balkanski, Y. J., Foreman-Fowler, M., Jones, D. B. A., Horowitz, L. W., Fusco, A. C., Brenninkmeijer, C. A. M., Prather, M. J., Wofsy, S. C., and McElroy, M. B.: Three-dimensional climatological distribution of tropospheric OH: Update and evaluation, Journal of Geophysical Research: Atmospheres, 105, 8931–8980, https://doi.org/10.1029/1999jd901006, https://doi.org/10.1029%2F1999jd901006, 2000.

Stremme, W., Grutter, M., Rivera, C., Bezanilla, A., Garcia, A. R., Ortega, I., George, M., Clerbaux, C., Coheur, P.-F., Hurtmans, D., Hannigan, J. W., and Coffey, M. T.: Top-down estimation of carbon monoxide emissions from the Mexico Megacity based on FTIR measurements from ground and space, Atmospheric Chemistry and Physics, 13, 1357–1376, https://doi.org/10.5194/acp-13-1357-2013, https://www.atmos-chem-phys.net/13/1357/2013/, 2013.

Varon, D. J., Jacob, D. J., McKeever, J., Jervis, D., Durak, B. O. A., Xia, Y., and Huang, Y.: Quantifying methane point sources from fine-scale satellite observations of atmospheric methane plumes, Atmospheric Measurement Techniques, 11, 5673–5686, https://doi.org/10.5194/amt-11-5673-2018, https://www.atmos-meas-tech.net/11/5673/2018/, 2018.

Veefkind, J., Aben, I., McMullan, K., Förster, H., de Vries, J., Otter, G., Claas, J., Eskes, H., de Haan, J., Kleipool, Q., van Weele, M., Hasekamp, O., Hoogeveen, R., Landgraf, J., Snel, R., Tol, P., Ingmann, P., Voors, R., Kruizinga, B., Vink, R., Visser, H., and Levelt, P.: TROPOMI on the ESA Sentinel-5 Precursor: A GMES mission for global observations of the atmospheric composition for climate, air quality and ozone layer applications, Remote Sensing of Environment, 120, 70–83, https://doi.org/10.1016/j.rse.2011.09.027, https://doi.org/10.1016%2Fj.rse.2011.09.027, 2012.

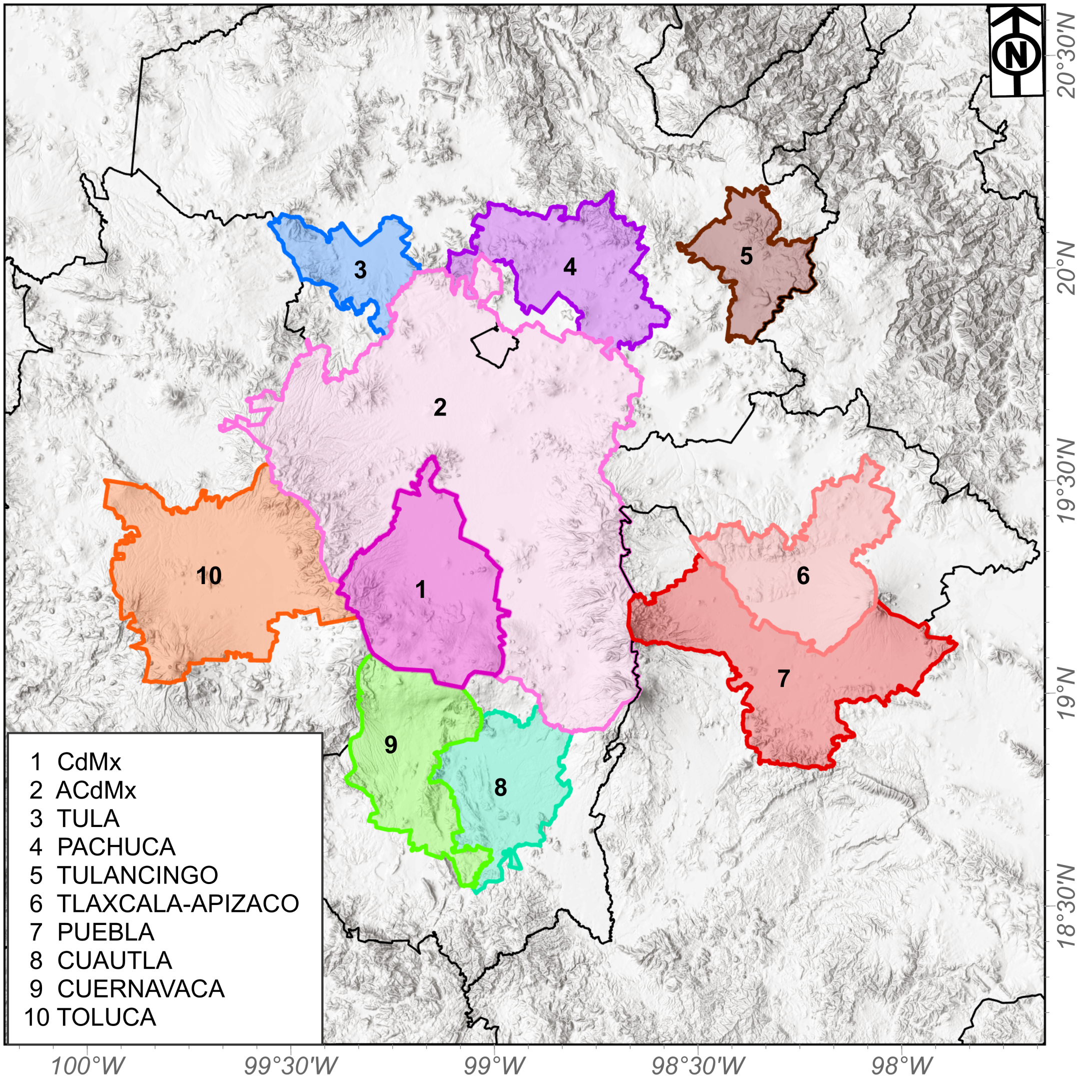

Figure 1. Urban districts surrounding Mexico City. For each of the color coded domains a separate ~~WRF~~ WRF-chem tracer run was performed based on the emissions within the polygons. The elevation map in the background is under copyright © Esri, Airbus DS, USGS, NGA, NASA, CGIAR, N Robinson, NCEAS, NLS, OS, NMA, Geodatastyrelsen, Rijkswaterstaat, GSA, Geoland, FEMA, Intermap and the GIS user community.

Vidot, J., Landgraf, J., Hasekamp, O., Butz, A., Galli, A., Tol, P., and Aben, I.: Carbon monoxide from shortwave infrared reflectance measurements: A new retrieval approach for clear sky and partially cloudy atmospheres, Remote Sensing of Environment, 120, 255–266, https://doi.org/10.1016/j.rse.2011.09.032, https://doi.org/10.1016%2Fj.rse.2011.09.032, 2012.

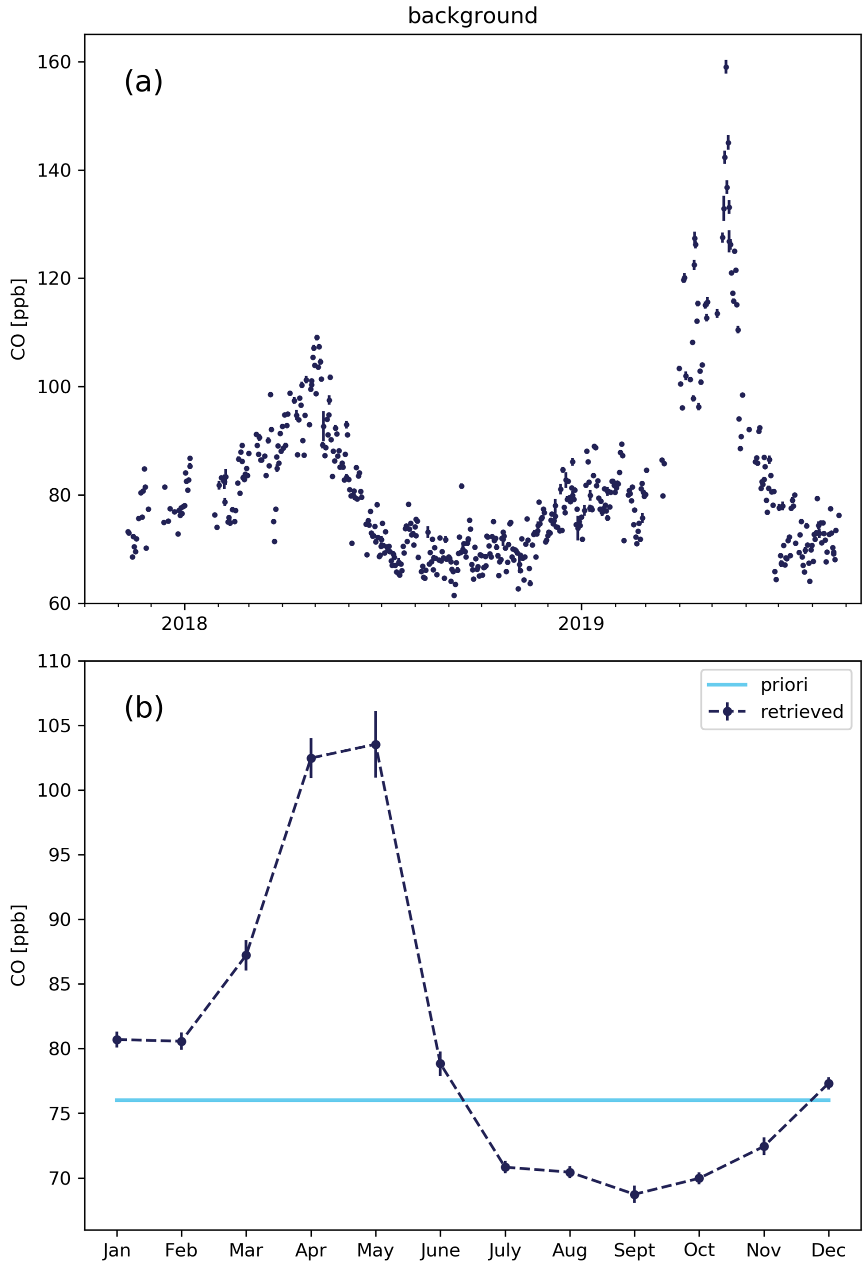

Figure 2. Background CO concentration for the domain shown in Fig. 1 estimated by fitting the ~~WRF~~ WRF-chem simulation to the TROPOMI data. (a) background CO for individual collocations from the 9th of November 2017 to the 25th of August 2019. (b) Monthly mean background CO based on the individual collocations. The error bars are the standard error of the mean and the light blue line time invariant prior used in the fit.

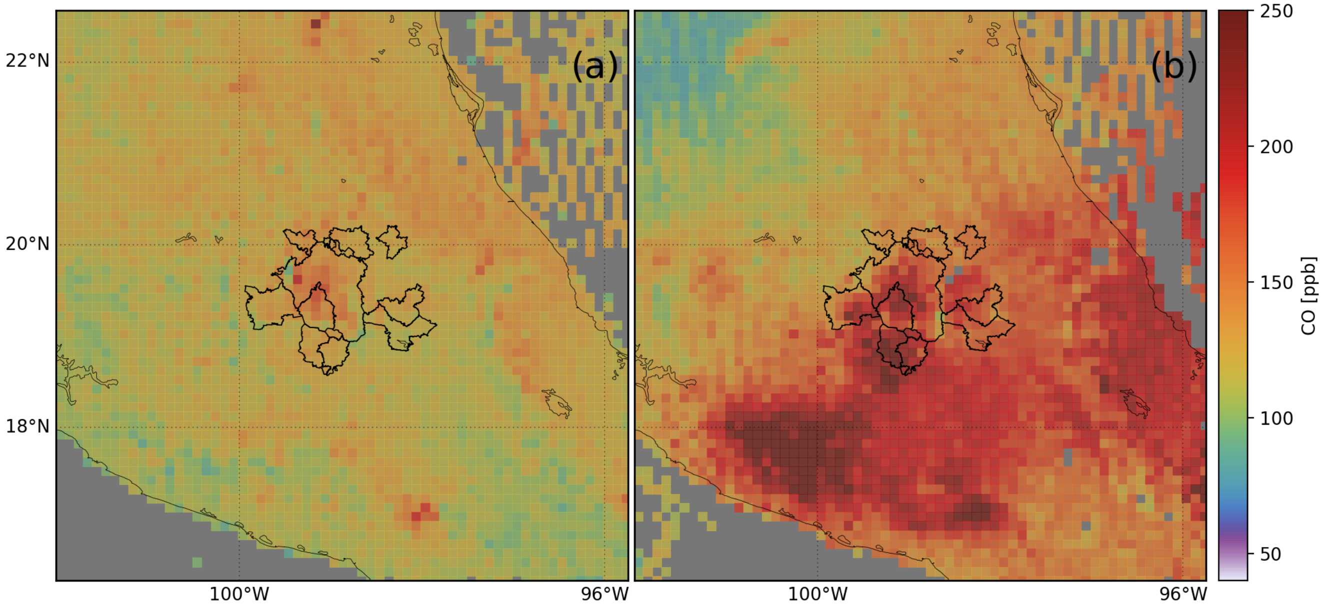

Figure 3. TROPOMI CO data over Mexico City averaged on a 0.1 by 0.1 degree lat/lon grid. (a) averaged from 12 to 18 of April 2019 showing undisturbed background CO levels. (b) averaged from 12 - 18 of May 2019 showing high CO concentrations in Mexico City caused by fires in the South-East. The street map in the background is under copyright © 2009 ESRI, AND, TANA, ESRI Japan, UNEP-WCMC.

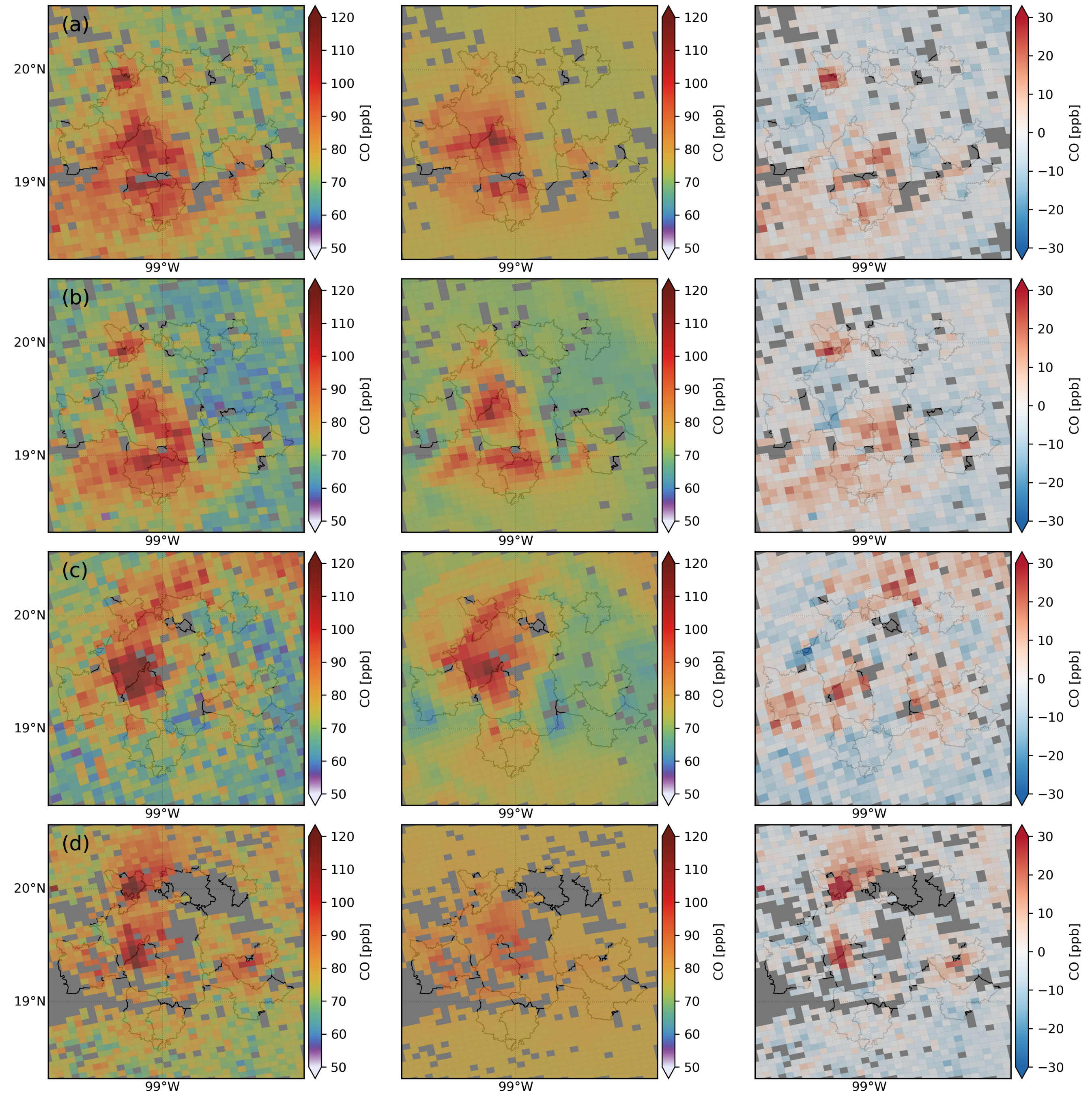

Figure 4. Example cases for fitting the ~~WRF~~ WRF-chem simulation to the TROPOMI data deploying the "Final-fit" approach for (a) the 20th of September, (b) the 7th of November, (c) the 19th of November 2018 and (d) the 17th of August 2019. TROPOMI CO retrievals (left column), ~~WRF~~ WRF-chem simulation fitted to the TROPOMI data (middle column), and the residual (right column, TROPOMI - ~~WRF~~WRF-chem).

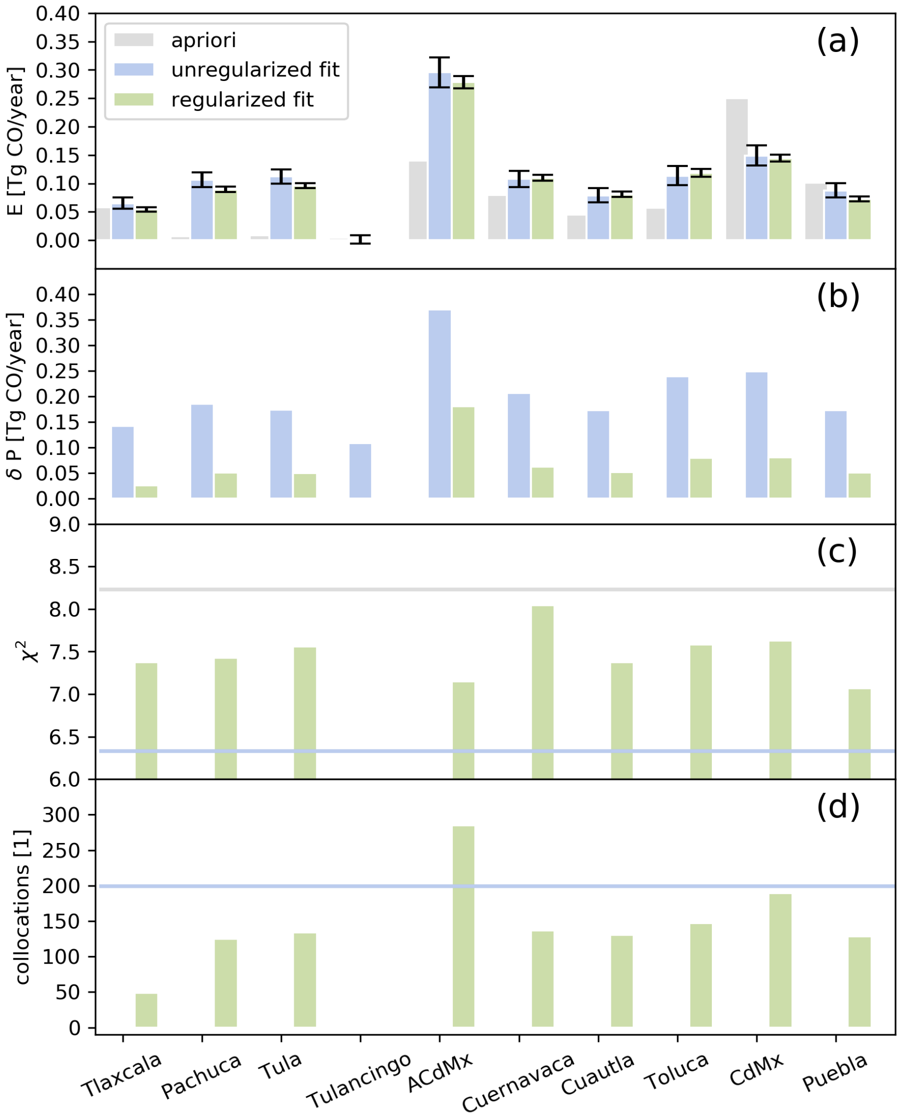

Figure 5. Statistics of CO emissions averaged from the 9th of November 2017 to the 25th of August 2019 for the tracer domains shown in Fig. 1. (a) Median of the priori emissions (adapted INEM inventory) used for the ~~WRF~~ WRF-chem simulation (grey) and retrieved from the TROPOMI data (~~Pre-fit~~ unregularized fit in blue, ~~Final-fit~~ regularized fit in green). The error bars indicate the standard error of the mean calculated from the delta percentiles (b) used as a robust estimation of the standard deviation, (c) the median of the goodness of the fit (χ^2), and the number of collocations (~~c~~d). The number of collocation and the χ^2 values of the ~~Pre-fit is~~ apriori simulation and unregularized fit are the same for all tracer domains (blue and grey line) but in the ~~Final-fit~~ final regularized fit it is changing due to the information content filtering. Here, a collocation corresponds to a specific day because TROPOMI overpasses the region only once.

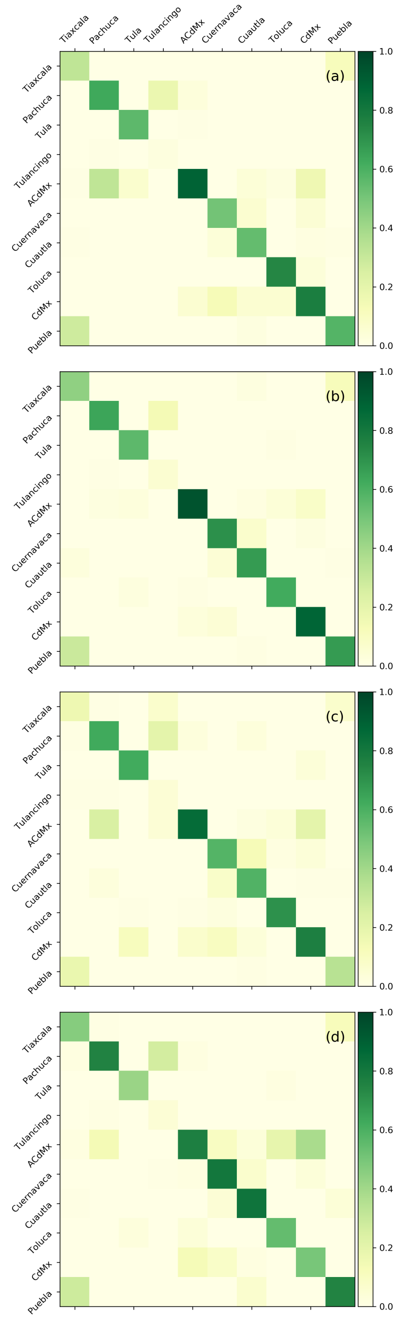

Figure 6. Averaging kernel matrices showing the sensitivity and cross-sensitivities for the scaling of the different tracer fields. The same cases as in Fig. 4 are shown for the dates (a) the 20th of September, (b) the 7th of November, (c) the 19th of November 2018 and (d) the 17th of August 2019 but deploying the regularized retrieval.

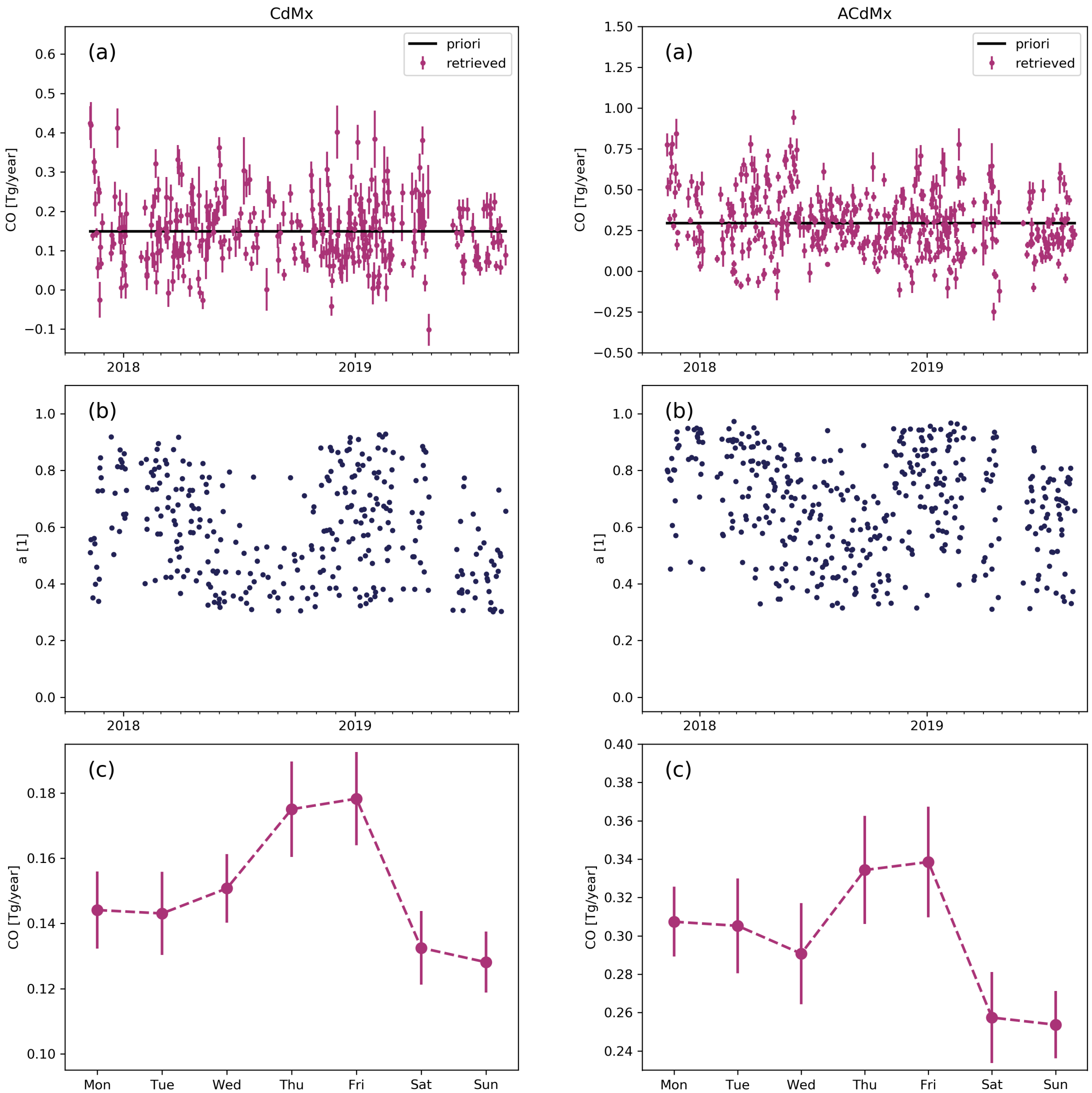

Figure 7. Retrieved CO Emissions from the TROPOMI data for the tracers ~~CDMX~~ CdMx (left panel) and ~~ACDMX~~ ACdMx (right panel). (a) Time series of individual retrieved CO emissions. The error bars indicate the error of the fit and the black line is the time invariant priori used in the fit. (b) degree of freedom of the scaling factor for the tracer field. Only data with dofs > 0.3 is accounted for. (c) Weekly cycle of the CO emissions. Median values are shown and the error bars are the standard error of the mean deploying the delta percentile as a robust estimation of the standard deviation.

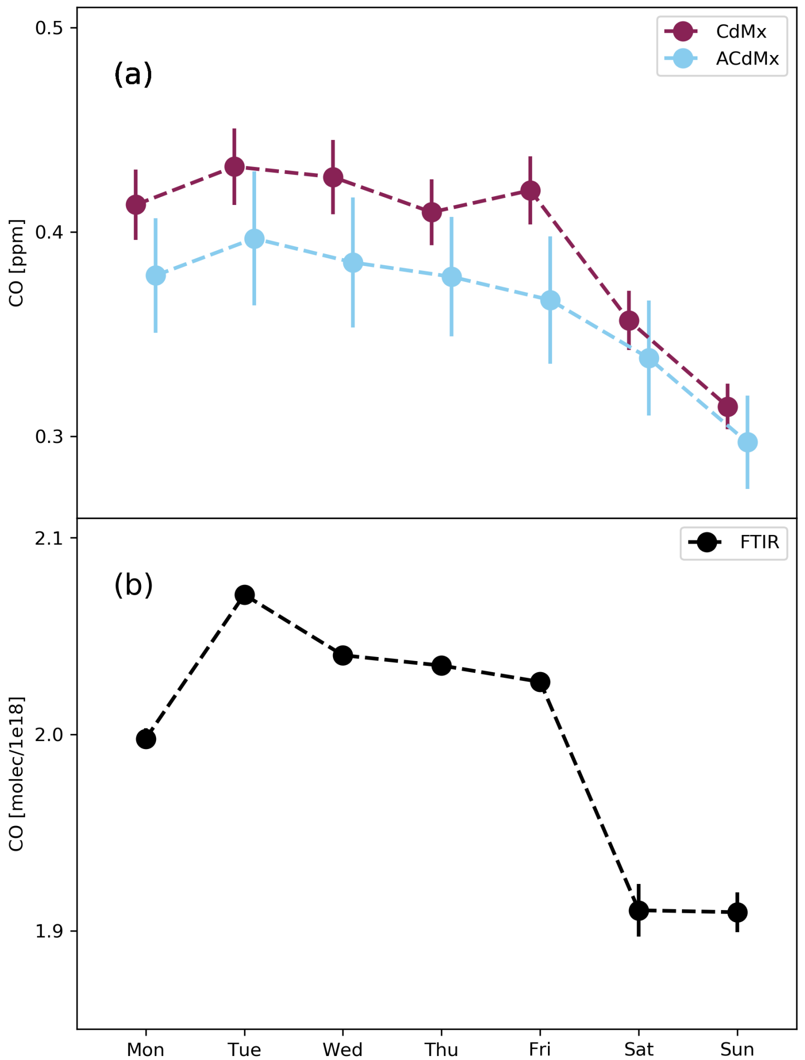

Figure 8. Weekly cycle of the CO concentration. (a) based on 29 ~~in situ~~ in-situ measurements station operated by SEDEMA. (b) ground-based FTIRs vertical column measurements of an instrument located in Mexico. Median values are shown and the error bars are the standard error of the mean deploying the delta percentile as a robust estimation of the standard deviation.